2007-03

# Simulation of coherent signals with forward error correction coding

Kong, Der-Hung

Monterey, California. Naval Postgraduate School


# NAVAL POSTGRADUATE SCHOOL

**MONTEREY, CALIFORNIA**

# THESIS

**SIMULATION OF COHERENT SIGNALS WITH FORWARD ERROR CORRECTION CODING**

by

Der-Hung Kong

March 2007

Thesis Advisor: Clark Robertson
Second Reader: Frank Kragh

**Approved for public release; distribution is unlimited.**

THIS PAGE INTENTIONALLY LEFT BLANK

| REPORT DOCUMENTATION PAGE | | | Form Approved OMB No. 0704-0188 |
|---|---|---|---|
| Public reporting burden for this collection of information is estimated to average 1 hour per response, including the time for reviewing instruction, searching existing data sources, gathering and maintaining the data needed, and completing and reviewing the collection of information. Send comments regarding this burden estimate or any other aspect of this collection of information, including suggestions for reducing this burden, to Washington headquarters Services, Directorate for Information Operations and Reports, 1215 Jefferson Davis Highway, Suite 1204, Arlington, VA 22202-4302, and to the Office of Management and Budget, Paperwork Reduction Project (0704-0188) Washington DC 20503. | | | |
| **1. AGENCY USE ONLY *(Leave blank)*** | **2. REPORT DATE** March 2007 | **3. REPORT TYPE AND DATES COVERED** Master's Thesis | |
| **4. TITLE AND SUBTITLE:** Simulation of Coherent Signals with Forward Error Correction Coding | | | **5. FUNDING NUMBERS** |
| **6. AUTHOR(S) : Der-Hung Kong** | | | |
| **7. PERFORMING ORGANIZATION NAME(S) AND ADDRESS(ES)** Naval Postgraduate School Monterey, CA 93943-5000 | | | **8. PERFORMING ORGANIZATION REPORT NUMBER** |
| **9. SPONSORING /MONITORING AGENCY NAME(S) AND ADDRESS(ES)** N/A | | | **10. SPONSORING/MONITORING AGENCY REPORT NUMBER** |
| **11. SUPPLEMENTARY NOTES** The views expressed in this thesis are those of the author and do not reflect the official policy or position of the Department of Defense or the U.S. Government. | | | |
| **12a. DISTRIBUTION / AVAILABILITY STATEMENT** Approved for public release; distribution is unlimited | | | **12b. DISTRIBUTION CODE** |


**13. ABSTRACT (maximum 200 words)**

This thesis focuses on the modeling and simulation of the performance of M-ary modulation techniques. In addition to the most popular used coherent modulation schemes, forward error correction (FEC) coded signals, and fading channels are also considered. The channel is modeled for the two cases of fading and no fading, both with additive white Gaussian noise (AWGN). The effect of barrage noise interference is also considered. Binary phase-shift keying (BPSK), 16-PSK, and 16-QAM (quadrature amplitude modulation) communication systems are simulated and analyzed. For BPSK, both hard decision decoding (HDD) and soft decision decoding (SDD) are considered. For 16-PSK and 16-QAM, only HDD is examined. Simulation results and analytical results are compared. The results show that the modeling and simulation in SystemView, are in excellent agreement with the analytical results.


| **14. SUBJECT TERMS** forward error correction (FEC), additive white Gaussian noise (AWGN), binary phase-shift keying (BPSK), QAM (quadrature amplitude modulation), hard decision decoding (HDD), soft decision decoding (SDD), SystemView | | | **15. NUMBER OF PAGES** 67 |
|---|---|---|---|
| | | | **16. PRICE CODE** |
| **17. SECURITY CLASSIFICATION OF REPORT** Unclassified | **18. SECURITY CLASSIFICATION OF THIS PAGE** Unclassified | **19. SECURITY CLASSIFICATION OF ABSTRACT** Unclassified | **20. LIMITATION OF ABSTRACT** UL |

NSN 7540-01-280-5500 Standard Form 298 (Rev. 2-89)
Prescribed by ANSI Std. 239-18

THIS PAGE INTENTIONALLY LEFT BLANK

**Approved for public release; distribution is unlimited**

# SIMULATION OF COHERENT SIGNALS WITH FORWARD ERROR CORRECTION CODING

Der-Hung Kong
Major, Taiwan R.O.C. Army
B.S., National Defense University, Chung Cheng Inst. of Tech., 1993

Submitted in partial fulfillment of the
requirements for the degree of

**MASTER OF SCIENCE IN ELECTRICAL ENGINEERING**

from the

**NAVAL POSTGRADUATE SCHOOL**
**March 2007**

Author: Der-Hung Kong

Approved by: Clark Robertson
Thesis Advisor

Frank Kragh
Second Reader

Jeffrey B. Knorr
Chairman, Department of Electrical and Computer Engineering

THIS PAGE INTENTIONALLY LEFT BLANK

# ABSTRACT

This thesis focuses on the modeling and simulation of the performance of M-ary modulation techniques. In addition to the most popular used coherent modulation schemes, forward error correction (FEC) coded signals, and fading channels are also considered. The channel is modeled for the two cases of fading and no fading, both with additive white Gaussian noise (AWGN). The effect of barrage noise interference is also considered. Binary phase-shift keying (BPSK), 16-PSK, and 16-QAM (quadrature amplitude modulation) communication systems are simulated and analyzed. For BPSK, both hard decision decoding (HDD) and soft decision decoding (SDD) are considered. For 16-PSK and 16-QAM, only HDD is examined. Simulation results and analytical results are compared. The results show that the modeling and simulation in SystemView, are in excellent agreement with the analytical results.

THIS PAGE INTENTIONALLY LEFT BLANK

# TABLE OF CONTENTS

# LIST OF FIGURES

# LIST OF TABLES

THIS PAGE INTENTIONALLY LEFT BLANK

# ACKNOWLEDGMENTS

After several years struggle, the thesis finally comes to conclusion. Two fundamental ingredients are necessary for any enterprise success and out of control of those who are directly endeavoring: support and confidence from third parties. I am extremely grateful to those who supported and trusted me during the accomplishment of this thesis and would like to acknowledge them here.

To my beloved wife, Joan Chen, for always believing me, for her kind support and for overcoming my absences during the hard times of research.

To my three children, Anita, Jeff, and Jacky, for the daily inspiration of their smile and for respecting my study moments.

To all my friends in Kuang-Hwa program, SDC division, CSIST, for the warm concern and encouragement. Especial thanks to Captain Chen, chief section leader in planning section, KH program, and Colonel Chu, former director in material and acquisition section, SMC division.

To my advisor, Professor Clark Robertson, for his knowledge, straightforward guidance, incentive, confidence and distinction that he treated me during the accomplishment of this thesis. There are many thanks need to say. I am not the man of great attainments in English. All I can say is my appreciation to Sir, you is beyond description.

To my thesis second reader, Assistant Professor Frank Kragh, for his attentiveness in every detail about my thesis.

Finally, I express my respect and acknowledgement to the CSIST, Taiwan ROC for honoring me with the rare opportunity and the sponsorship of these two years of studies at the Naval Postgraduate School.

THIS PAGE INTENTIONALLY LEFT BLANK

# EXECUTIVE SUMMARY

The purpose of this thesis is to model and simulate the most commonly used coherent systems, such as binary phase-shift keying (BPSK), 16-PSK, and 16-QAM (quadrature amplitude modulation) for different kinds of noisy and fading channels in order to develop a mechanism to evaluate the performance of these systems for conditions that do not easily yield to analysis. This is important because these coherent modulations are used in many communication systems including the sub-carriers in Orthogonal Frequency Division Multiplexed communications systems such as IEEE 802.11a, g, and n WLANs and the Joint Tactical Radio System Wideband Networking Waveform. Therefore, in order to predict the performance of these systems, simulations typified by the simulations in this thesis are necessary. SystemView provides a method to simulate the performance of communication systems that are otherwise difficult to analyze. In this thesis, coherent modulation schemes with forward error correction (FEC) coded signals transmitted over fading channels are simulated. The channel is modeled for both fading and no fading with additive white Gaussian noise (AWGN). The effects of barrage noise interference are also considered. BPSK, 16-PSK, and 16-QAM communication systems are simulated and analyzed. For BPSK, both hard decision decoding (HDD) and soft decision decoding (SDD) are considered. For 16-PSK and 16-QAM, only HDD is examined.

In order to verify the modeling and simulation procedure, the performance of coherent systems with no coding was examined first. Next, the performance of coherent systems with error correction coding was examined. Both hard and soft decision decoding was considered for binary systems, but only hard decision decoding was considered for non-binary systems. Finally, fading channels were also considered.

Two major problems were found during the modeling and simulation. First, the total number of samples is restricted to $2^{31}$ (= 2,147,483,647) for all simulation loops, which reduces accuracy for high signal-noise-ratios (SNRs). Next, too much CPU

resource is required to conduct each simulation. These restrictions are an artifact of using the student version of SystemView and presumably would not be as much of a drawback with the commercial version.

The performance of the coherent systems examined, both with and without coding, all agreed very well with analytical results. Since the simulations developed have been verified for the AWGN case, they can now be modified to examine cases that are not possible to evaluate by analysis.

# I. INTRODUCTION

## A. THESIS OBJECTIVE

Wireless local area networks (WLANs) are increasingly used for both commercial and military applications. The objective of this thesis is to investigate the performance of systems that use different combinations of modulation order and code rates of forward error correcting codes such as those typically used in WLANs implemented with orthogonal frequency-division multiplexing (OFDM). This thesis focuses on modeling and simulation of the performance of *M*-ary modulation with forward error correction (FEC) coded signals for both channel fading and no channel fading with additive white Gaussian noise (AWGN). Both hard decision decoding (HDD) and soft decision decoding (SDD) are considered. Since the analysis with SDD is not exact when using non-binary modulation and a binary code, it is important to verify approximate analytical approaches by simulation.

## B. RELATED RESEARCH

Wireless communications have ushered in a new era. Numerous studies have investigated the performance of OFDM for many different fading channels, such as OFDM over frequency-nonselective, fast Rayleigh and Ricean fading channels in [1] and [2], frequency-selective, Rayleigh fading channels in [3], frequency-selective, slow Ricean fading channels in [4], frequency-selective, slow Nakagami fading channels in [5], and frequency-selective, slow Nakagami fading channel with pulsed jamming in [6]. Theses papers derived analytical expressions for the different channel characteristics. These are just a few of many related studies. Distinct from the above works, in this thesis, we focus on the modeling and simulation of the performance of *M*-ary modulation with FEC coded signals over fading channels. The channel is modeled for the two cases of fading and no fading, both with AWGN. Binary phase-shift keying (BPSK), 16-PSK, and 16-QAM (quadrature amplitude modulation) communication systems are simulated and analyzed.

## C. THESIS ORGANIZATION

After the introduction, the thesis is organized into five remaining chapters. Following an introduction, Chapter II introduces the fundamental background of the digital communication system, including the modulation techniques. Fading channels are discussed in Chapter III. Forward error correction (FEC) is also introduced in this chapter. Next, Chapter IV explores the differences between simulation results and the analytical results. The use of SystemView software to simulate the system under investigation is also discussed in this chapter. Finally, Chapter V is a summary and recommendation for future work.

## D. REQUIRED SOFTWARE

SystemView by Elanix, version 5.0 was used to build and conduct the simulations. MATLAB version 7.1.0 (R14) was used to generate the diagrams.

# II. DIGITAL COMMUNICATION SYSTEM

Digital Communication has entered our daily lives in many different ways, for example, the radio and television sets in our living rooms and the networks around us. In this chapter, the fundamental background of digital communication, including various modulation techniques and fading channels are described.

## A. OVERVIEW

Digital communication can be simply thought of as a series of processes from information input, encoding, modulating, demodulating, decoding, and information recovery. The basic digital communication model is described in Figure 1.

With digital binary communication systems, one of two unique signals, say $s_1(t)$ or $s_2(t)$, which represent a bit "1" or a bit "0", are transmitted each bit duration. Normally, the signals may be represented as a time sequences of symbols, where there are $M$ distinct symbols, and each symbol represents $q$ bits of information. Consequently, the relation between symbol alphabet size $M$, and $q$ bits of information can be expressed as,

$$q = \log_2 M \tag{2.1}$$

or

$$2^q = M \tag{2.2}$$

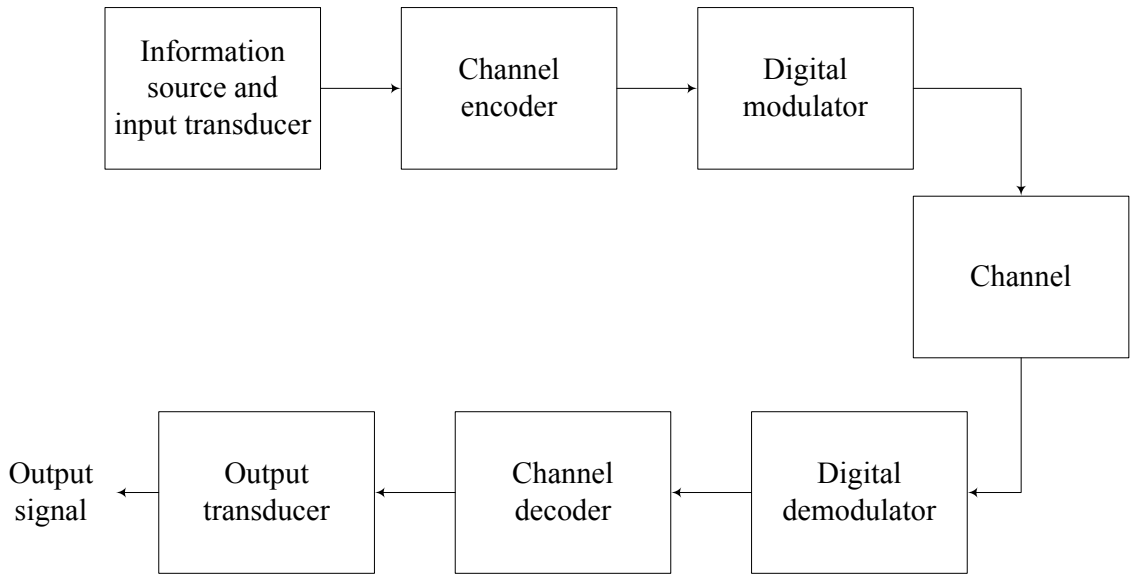


Figure 1. Digital Communication Model (After Ref. 7)

Shannon's theorem says that for an arbitrarily small probability of error, the maximum possible bandwidth efficiency is limited by the noise in the channel [8]. For a channel with AWGN, the capacity can be stated as [9]

$$C = W \log_2 \left( 1 + \frac{P_C}{P_n} \right) \tag{2.3}$$

or

$$C = W \log_2 \left( 1 + \frac{E_b C}{N_0 W} \right) \tag{2.4}$$

where $C$ is the channel capacity in bits/s, $P_C$ is the average received signal power, $P_n$ is the average received noise power, $E_b$ is the average received signal energy per bit, $W$ is the noise equivalent system bandwidth in Hz, and $N_0 / 2$ is the noise power spectral density (PSD) in W/Hz.

For a certain $E_b / N_0$, Shannon's theorem states that if $C \geq R_b$, where $R_b$ is the bit rate, then it is possible to achieve error free communication. On the contrary, if $R_b > C$, then error free communication is not possible. For a general expression, Equation (2.4) was modified as follows:

$$\frac{E_b}{N_0} = \frac{1}{C/W}(2^{C/W} - 1) \tag{2.5}$$

This equation is typically plotted on the bandwidth efficiency plane ( $R_b / W$ versus $E_b / N_0$ ) [11] as shown in Figure 2. If $R_b$ is the data rate in bits per second and $W$ is the bandwidth occupied by the modulated radio frequency (RF) signal, then bandwidth efficiency $\eta_B$ is expressed as [10]

$$\eta_B = \frac{R_b}{W} \tag{2.6}$$

According to this equation above, there are two different regions on this bandwidth-efficiency plane. The bandwidth-limited region has $\eta_B > 1$. The power-limited region has $\eta_B < 1$.

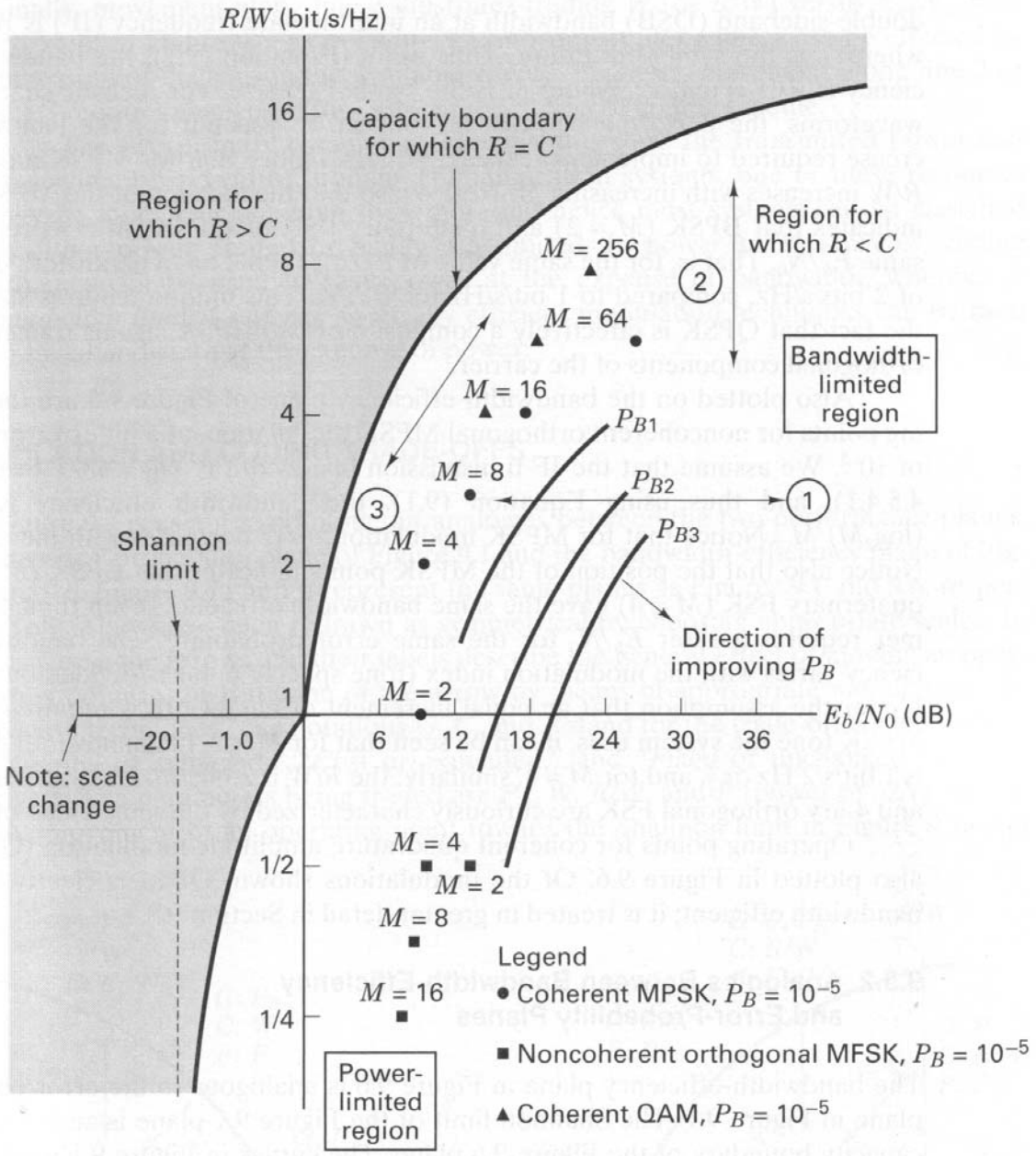


Figure 2. Bandwidth-efficiency plane (From Ref. 8)

## B. MODULATION TECHNIQUES

### 1. Binary Phase-Shift Keying (BPSK)

In binary phase-shift keying modulation, it represents a bit "1" or a bit "0" by changing the phase of the waveform, either zero or π radians (180$^{o}$), respectively. The waveform with this sudden phase change is shown in Figure 3.

A general transmission signal is

$$s(t) = \sqrt{2}A_C \cos\left[2\pi f_c t + \theta_d(t) + \theta_o\right] \tag{2.7}$$

where $2\pi f_c$ is the carrier frequency in radians/s, $\theta_d(t)$ represents the data, and $\theta_o$ is the fixed reference phase. Frequently, $\theta_d(t) = 0$ is used to represent bit "1", while $\theta_d(t) = \pi$ is used to represent bit "0".

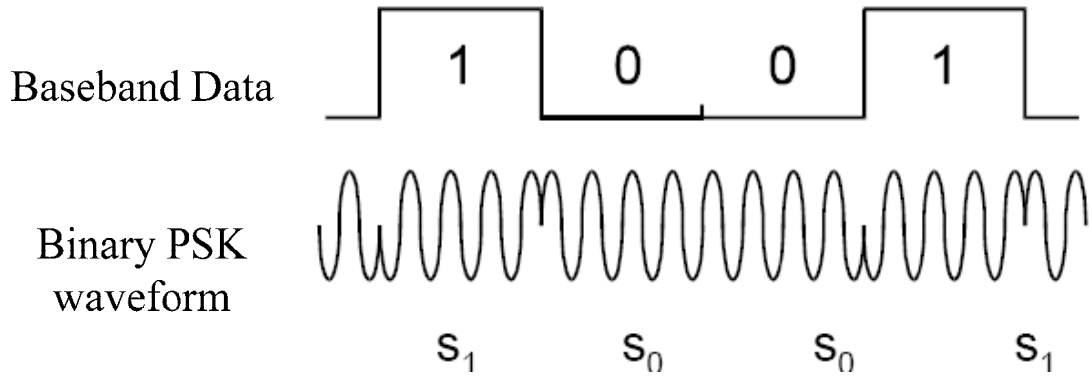


Figure 3. Data and waveform format for BPSK (After Ref. 12)

**2. Multi-level (M-ary) Phase and Amplitude**

***a. M-ary Phase Shift Keying (MPSK)***

On the bandwidth limited region, a frequently used modulation format is *M*-ary phase-shift keying (MPSK). The transmission signal of the $i^{th}$ symbol is

$$s(t) = \sqrt{2}A_C \cos\left[2\pi f_c t + \frac{2\pi(m-1)}{M} + \theta_o\right] \tag{2.8}$$

where $m = 1, 2, \ldots, M$.

Unlike BPSK which only utilizes the in-phase component, MPSK uses both in-phase and the quadrature components.

***b. M-ary Quadrature Amplitude Modulation (MQAM)***

The constellations for both 16QAM and 16PSK are shown in Figure 4. In *M*QAM, amplitude and phase-shift keying are combined to transmit several bits per symbol (in this case $q = 4$ bits/symbol).

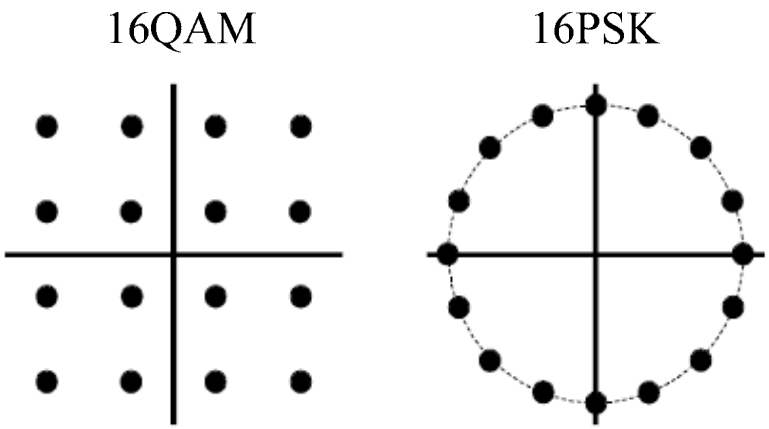


Figure 4. The constellation of 16QAM and 16PSK (After Ref. 12)

In this chapter, digital communication systems were introduced and modulation schemes such as BPSK, MPSK and MQAM were discussed. In the next chapter, the primary sources of channel interference are considered and error correction coding is introduced.

# III. FADING CHANNELS AND ERROR CORRECTION CODING

*Additive white Gaussian noise* (AWGN) is always present in all communication systems and affects each transmitted symbol *independently* [11]. In addition to AWGN, the focus of this chapter is on fading channels and error correction coding.

## A. FADING CHANNELS

Reflection, diffraction, and scattering are the main physical factors that affect the signals to be received. Due to these factors radio frequency channels are extremely random and are not easily analyzed. Many wireless communication channels do not have a line-of-sight (LOS) signal path. When there is no LOS, the signal is only received by *multipath*; that is, there are multiple signal paths from the transmitter to the receiver as a result of reflection, diffraction, and scattering of the original signal.[11] Multipath is illustrated in Figure 5.

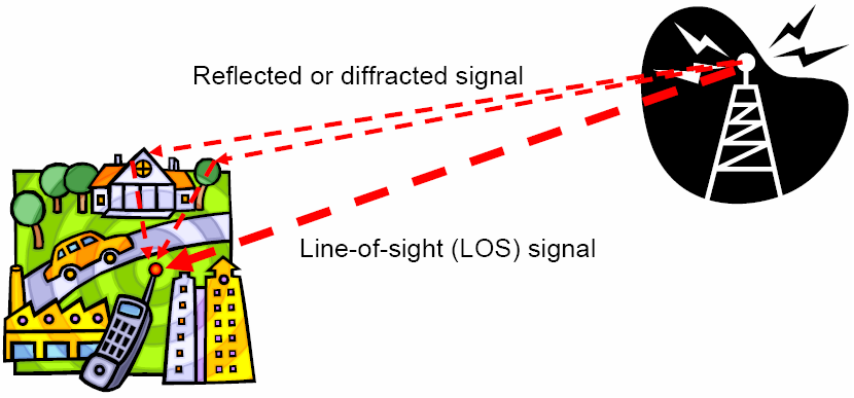


Figure 5. Multipath propagation

Multipath can cause large fluctuations in the received signal's amplitude, phase, and angle of arrival. Figure 6 represents an overview of how fading-channel can be categorized. Large-scale fading relates received signal strength for large changes in transmitter and receiver separation distance (usually much bigger than signal's wavelength). Small-scale fading (changes in separation distances on the order of a half wavelength) is used to describe the rapid fluctuation of the amplitude of the received signal over a short period of time, and large-scale fading effects may be ignored. [11]

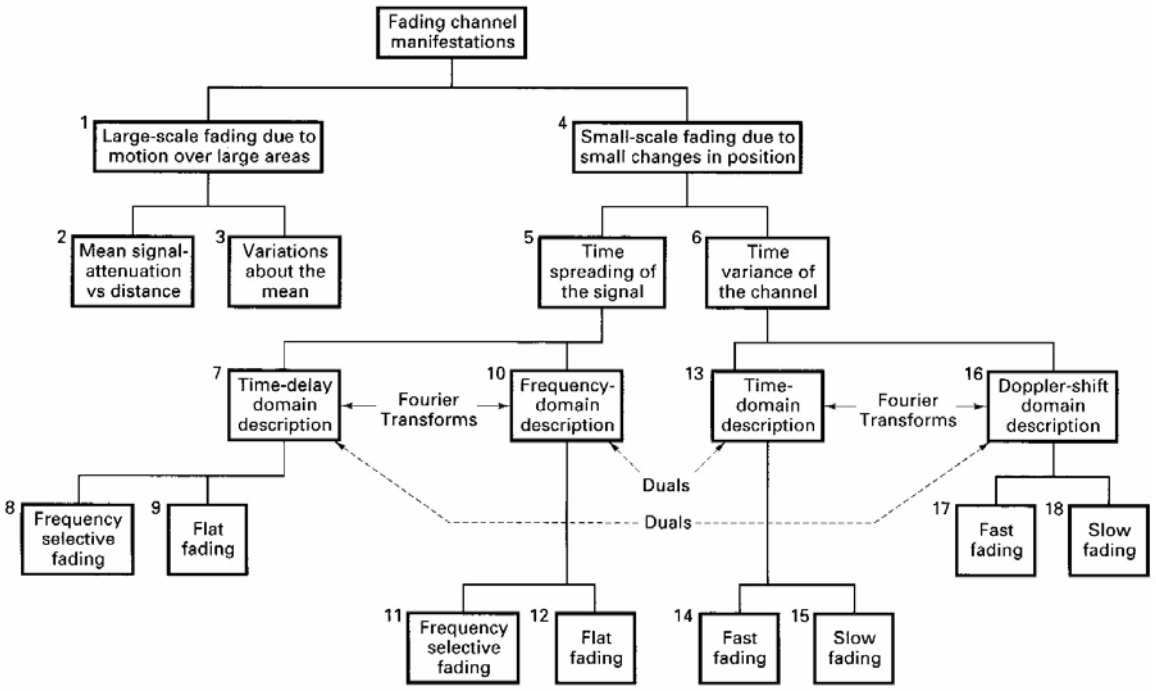


Figure 6. Fading-channel manifestations (From Ref. 11)

## B. SMALL-SCALE FADING

The distance between small-scale fades is on the order of $\lambda/2$, as shown in Figure 7. As Figure 6 shows, the two main mechanisms that cause small-scale fading are time spreading of the signal due to multipath and time variance of the channel due to Doppler spread.

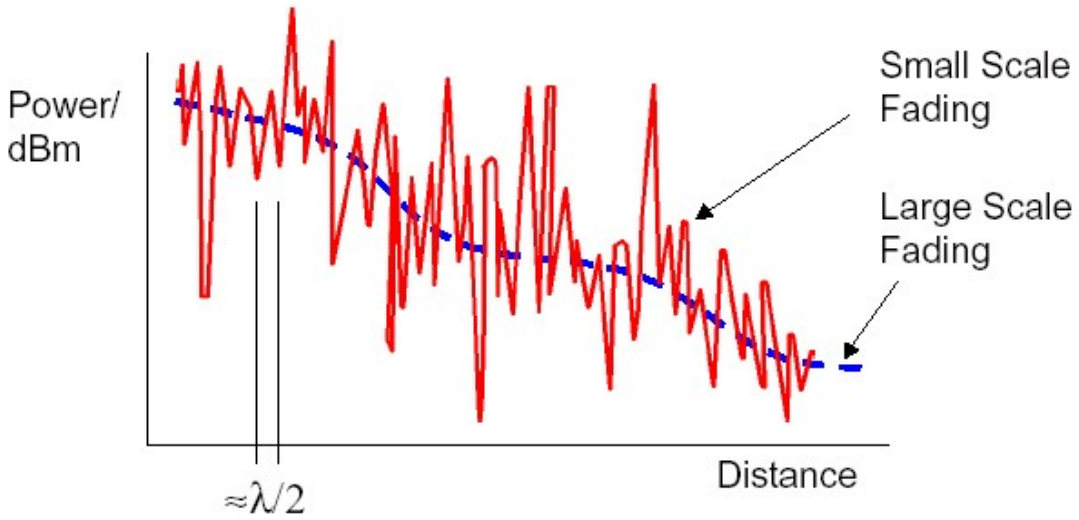


Figure 7. Large and small scale fading (From Ref. 13)

### 1. Time Spreading of the Signal Due to Multipath

As shown in Figure 6, time spreading of the signal will can be due to either frequency-selective fading or frequency nonselective fading (flat fading). The coherence bandwidth $f_0$ and the maximum excess delay $T_m$ are two factors used to describe fading. The reciprocal relationship between $f_0$ and $T_m$ is given by [11]

$$f_0 \approx \frac{1}{T_m} \tag{3.1}$$

where the time $T_m$ represents the maximum excess delay, or the difference of arrival times of the first and the last received signal components.

Typically, the received signal consists of several different multipath components, which causes the average received power $S(\tau)$ to present multiple isolated peaks, as illustrated in Figure 8. [11]

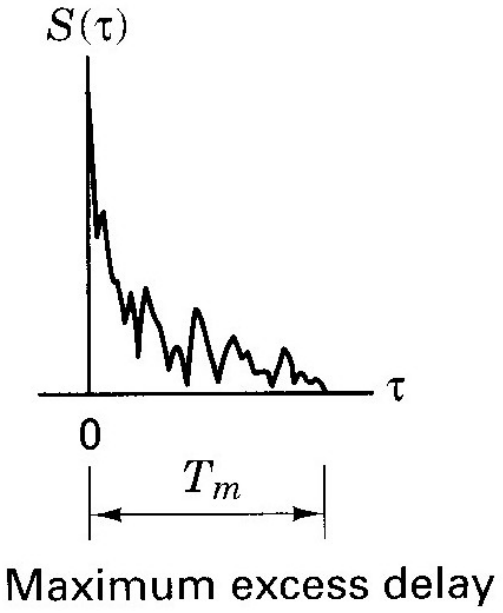


Figure 8. Multipath intensity profile (After Ref. 11)

The multipath intensity profile can change significantly for channels with the same value of $T_m$. A general parameter, the root-mean-square (rms) delay spread, was used instead of $T_m$, defined [11]

$$\sigma_\tau = \sqrt{\overline{\tau^2} - \bar{\tau}^2} \tag{3.2}$$

where $\bar{\tau}$ is the mean excess delay and $\overline{\tau^2}$ is the second moment of $\tau$.

There is no fixed relationship between $f_0$, the coherence bandwidth, and $\sigma_\tau$, the root-mean-square (rms) delay spread. If the coherence bandwidth is defined as the frequency interval over which the frequency correlation function has a correlation of at least 0.9, the coherence bandwidth is approximately [10]

$$f_0 \approx \frac{1}{50\sigma_\tau} \tag{3.3}$$

If the frequency correlation function is above 0.5, then the coherence bandwidth is empirically obtained. [14]

$$f_0 \approx \frac{1}{5\sigma_\tau} \tag{3.4}$$

#### *a. Frequency-Selective Fading*

For the frequency-selective case, if the coherence bandwidth $f_0$ is less than the symbol rate $1/T_S$; that is [11]

$$f_0 < \frac{1}{T_S} \approx W \tag{3.5}$$

which means

$$T_m > T_S \tag{3.6}$$

where the symbol rate $1/T_S$ is equal to the signaling rate. Figure 9(a) shows that various spectral components of the transmitted signal will be affected differently.

#### *b. Flat Fading*

Frequency-nonselective or flat-fading degradation appears whenever [11]

$$f_0 > W \tag{3.7}$$

or, equivalently,

$$T_m < T_S \tag{3.8}$$

Figure 9(b) illustrates that all of the spectral components of the transmitted signal are affected in approximately the same way.

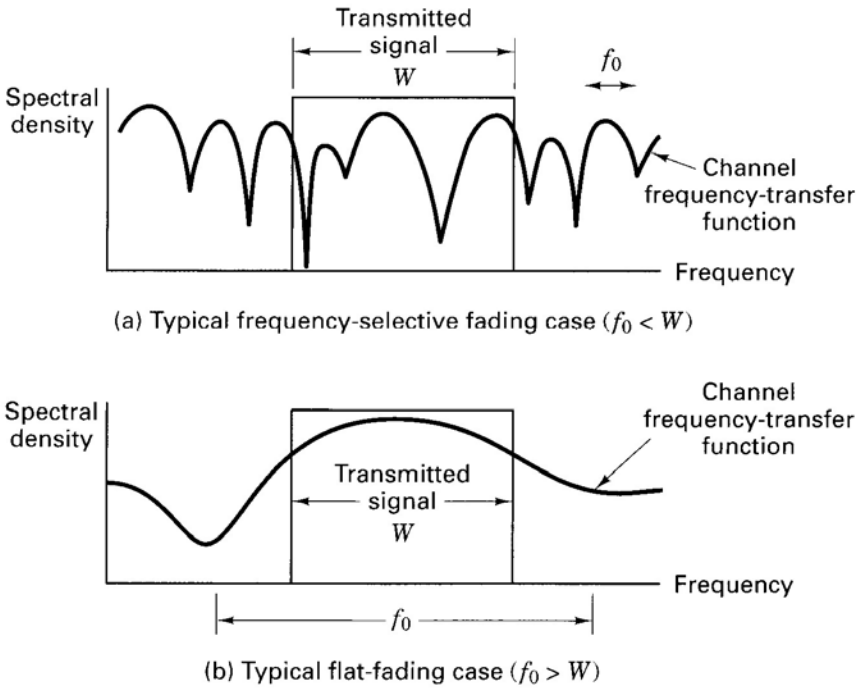


Figure 9. Typical cases for frequency-selective and flat-fading (From Ref. 11)

### 2. Time Variance of the Channel Due to Doppler Spread

There are two parameters used to describe the time-variant nature of the channel: *Doppler spread* $f_d$ and *coherence time* $T_0$.

The magnitude of the frequency shift $f_d$ is given by [11]

$$f_d = \frac{V}{\lambda} \tag{3.9}$$

where $V$ is relative velocity and $\lambda$ is the signal wavelength. When the transmitter and receiver comes to each other, $f_d$ is positive, and when they move away from each other, $f_d$ is negative.

The Doppler spread $f_d$ and the coherence time $T_0$ are reciprocally related. [11]

$$T_0 \approx \frac{1}{f_d} \tag{3.10}$$

***a. Fast Fading***

A channel is said to be fast fading if the symbol rate $1/T_S$ (approximately equal to the bandwidth $W$) is less than the fading rate $1/T_0$ (approximately equal to $f_d$); that is, fast fading is characterized by [11]

$$W < f_d \tag{3.11}$$

or

$$T_S > T_0 \tag{3.12}$$

In practice, fast fading only occurs for low data rates [11].

***b. Slow Fading***

In the frequency domain, this implies that the Doppler spread of the channel is much less than the bandwidth of the baseband signals. That is [11]

$$W > f_d \tag{3.13}$$

or

$$T_S < T_0 \tag{3.14}$$

### 3. Summary of Small-Scale Fading

Depending on the relation between the signal parameters (such as bandwidth, symbol period, etc.) and the channel parameters (such as rms delay spread and Doppler spread), different transmitted signals will experience different types of fading. Signal time spreading (signal dispersion) and the time-variant nature of the channel are two mechanisms that result in small-scale fading. Figure 10 summarizes these two small-scale fading mechanisms. [11]

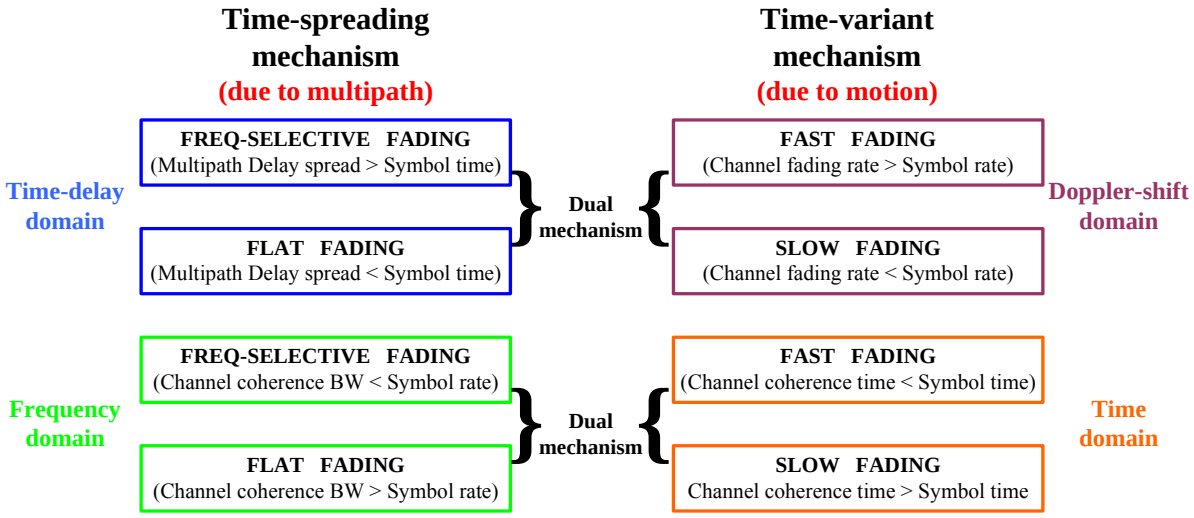


Figure 10. Summary of Small-scale fading (After Ref. 11)

## C. RAYLEIGH AND RICEAN CHANNELS

### 1. Rayleigh Fading Channel

In the Rayleigh fading case, there is no LOS signal transmitted between transmitter and receiver and all of the received signal power is due to multipath. For Rayleigh fading channels (a special case of the Ricean fading channel), the received amplitude is modeled as a Rayleigh random variable with the probability density function (pdf) given by [14]

$$p(r) = \frac{r}{\sigma^2} \exp\left( -\frac{r^2}{2\sigma^2} \right), \ (0 \le r \le \infty) \tag{3.15}$$

where $\sigma$ is the rms value of the received voltage signal before envelope detection and $\sigma^2$ is the time-average power of the received signal before envelope detection.

### 2. Ricean Fading Channel

When there is a dominant signal component present, such as a LOS signal, the effect of a LOS signal arriving with many weaker multipath signals gives rise to the Ricean distribution. The pdf of the Ricean distribution is given by [14]

$$p(r) = \frac{r}{\sigma^2} \exp\left[ -\frac{(r^2 + A^2)}{2\sigma^2} \right] I_0\left( \frac{Ar}{\sigma^2} \right), \ (A \geq 0, r \geq 0) \tag{3.16}$$

The parameter $A$ denotes the peak amplitude of the dominant signal and $I_0(\bullet)$ is the modified Bessel function of the first kind and zero-order.

The Ricean distribution is often described in terms of a parameter $\zeta$ (Ricean factor) [14], which is defined as the ratio between the deterministic LOS signal power and the non-LOS multipath signal power, given by $\zeta = A^2/(2\sigma^2)$, or in $dB$,

$$\zeta(dB) = 10 \log \frac{A^2}{2\sigma^2} dB \tag{3.17}$$

As $A \to 0, \zeta \to -\infty(dB)$, and as the dominant path decreases in amplitude, the Ricean distribution degenerates to a Rayleigh distribution.

## D. SUMMARY OF MULTIPATH FADING CHANNELS

The characteristic of the channel was described and multipath fading channels were discussed. The mechanisms and types of small scale fading channels, frequency-selective fading, flat fading, fast fading, and slow fading were also introduced. In this thesis, two widely used models for fading channels, the Rayleigh fading channel and the Ricean fading channel, are assumed. In the next section, error control coding is discussed.

## E. ERROR CORRECTION CODING

Error correction coding has made digital communications practical and popular. By using the error correction coding method, digital systems can easily detect and correct errors. All communication systems should be designed to combat the degenerative effects of the communication channel such as noise, interference, and fading.

There are two basic error control strategies: *automatic repeat request* (ARQ) and *forward error correction* (FEC) coding. Forward error correction coding consists of adding a certain number of redundant bits to the actual data bits in a particular pattern such that recovery of the actual data bits is enhanced. [11] In this thesis, FEC is used.

### 1. Forward Error Correcting (FEC) Coding

Forward error correction (FEC) coding consists of adding a certain number of redundancy bits to the actual data bits in a specified pattern such that recovery of the actual data bits is possible. The two primary types of forward error correction codes are block codes and convolutional codes.[11] In this thesis, convolutional codes are used.

In a system utilizing FEC coding, for every $k$ information data bits, $n$ coded bits are transmitted where $n > k$, the relation is,

$$nT_{b_C} = kT_b \tag{3.18}$$

where $T_{b_C}$ is the duration of a coded, or channel, bit and $T_b$ is the duration of a data bit. Therefore,

$$T_{b_C} = \frac{k}{n} T_b = rT_b \tag{3.19}$$

$$R_{b_C} = \frac{R_b}{r} \tag{3.20}$$

where the coded, or channel, bit rate is $R_{b_C} = 1/T_{b_C}$ and $r = k/n$ is the code rate.

Since $r < 1$, the coded bit rate is higher than the uncoded bit rate; and for a constant data bit rate, the addition of FEC coding increasing the bandwidth by the factor $n/k = 1/r$.

[11] Also, the average energy per coded bit is less than the average energy per uncoded bit; and for a fixed average energy per data bit, the addition of FEC coding increases the probability of channel bit error. [11]

The average transmitted power is the same whether coded or uncoded bits are transmitted:

$$E_{b_C} R_{b_C} = E_b R_b \tag{3.21}$$

Therefore,

$$E_{b_C} = rE_b \tag{3.22}$$

Coding gain is defined as the difference in the signal-to-noise ratios required by a FEC coded communication system and the same uncoded communication system to achieve a specific probability of bit error:

$$G_{dB} = \left(\frac{E_b}{N_0}\right)_{uncoded_{dB}} - \left(\frac{E_b}{N_0}\right)_{coded_{dB}} \tag{3.23}$$

### 2. Hard Decision Decoding (HDD) and Soft Decision Decoding (SDD)

In the process of decoding, two different types of "decisions" can be made in order to recover the original information. A "hard decision" can be made in which a received bit is demodulated as being either a binary one or zero. This determination is then sent to the Viterbi decoding algorithm for decoding of the actual information bits.

A "soft decision" may also be made in which the decoder allows for varying degrees of certainty that a received bit is a one or a zero. This quantization enables the decoder to classify a received bit as a "strong" binary one or zero or marginally declaring the bit a binary one or zero. This approach improves the ability of the decoder to accurately estimate a received bit's identity. [11]

In this chapter, fading channels and error correction coding were both discussed. In the next chapter, the differences between simulation results and the analytical results are compared.

# IV. COHERENT SYSTEM SIMULATION IN SYSTEMVIEW

## A. PERFORMANCE OF COHERENT SYSTEMS WITH NO CODING

### 1. Coherent Detection (BPSK, *M*PSK, *M*QAM)

In this subsection, the probability of bit error for binary phase-shift keying (BPSK), *M*-ary phase-shift keying (*M*PSK), and *M*-ary quadrature amplitude modulation (*M*QAM) waveforms transmitted over slow, flat fading channels is listed. The following equations and tables are summarized after [15].

For each of these signaling techniques, the conditional probability of bit error is of the form [15]

$$P_b(\gamma_S) = \frac{a}{q} Q\left(\sqrt{b\gamma_S}\right) \tag{4.1}$$

where $Q(\bullet)$ is the Q-function and $a$, $b$, and $q$ are constants that depend on the modulation type. The constants $a$, $b$, and $q$ for BPSK, *M*PSK, and *M*QAM are listed in Table 1. For *M*QAM with $q$ even, a square constellation is assumed, while for *M*QAM with $q$ odd, a rectangular constellation is assumed. For example, in Figure 11, $M = 8$ ($q$=3, blue line) yields a rectangular constellation and $M = 16$ ($q$=4, red line) has a square constellation.

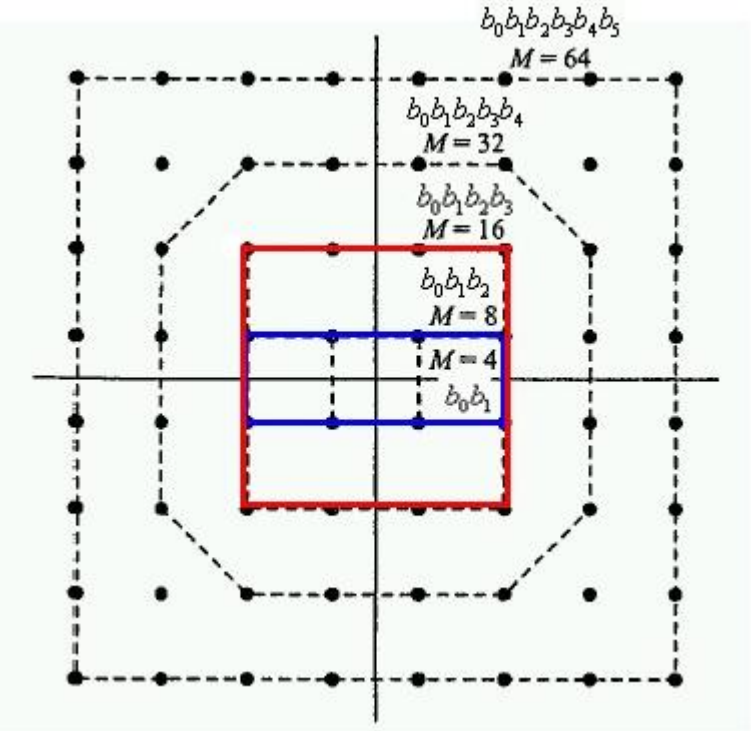


Figure 11. *M*QAM signal constellation (After Ref. 7).

Table 1. Modulation dependent constant for Equation (4.1) (After Ref. 15).

| Modulation | $q$ | $a$ | $b$ |
|---|---|---|---|
| BPSK | 1 | 1 | 2 |
| QPSK | 2 | 2 | 1 |
| *M*PSK | $\log_2 M$ | 2 | $2\cdot\sin^2(\pi/M)$ |
| *M*QAM | $4,6,8,\cdots$ | $4\cdot(1-2^{-q/2})$ | $3/(2^q-1)$ |
| *M*QAM | $3,5,7,\cdots$ | 4 | $3/(2^q-1)$ |

## 2. Model the Coherent System (BPSK, MPSK, MQAM) in SystemView

### *a. Simulation of BPSK in SystemView*

Baseband BPSK is the best binary modulation technique in terms of BER for channels with AWGN. In SystemView, a PN sequence generator is used to simulate the data source. Figures 12 and 13 show the simulation results for baseband BPSK, which shows good agreement with the analytical result in equation (4.1).

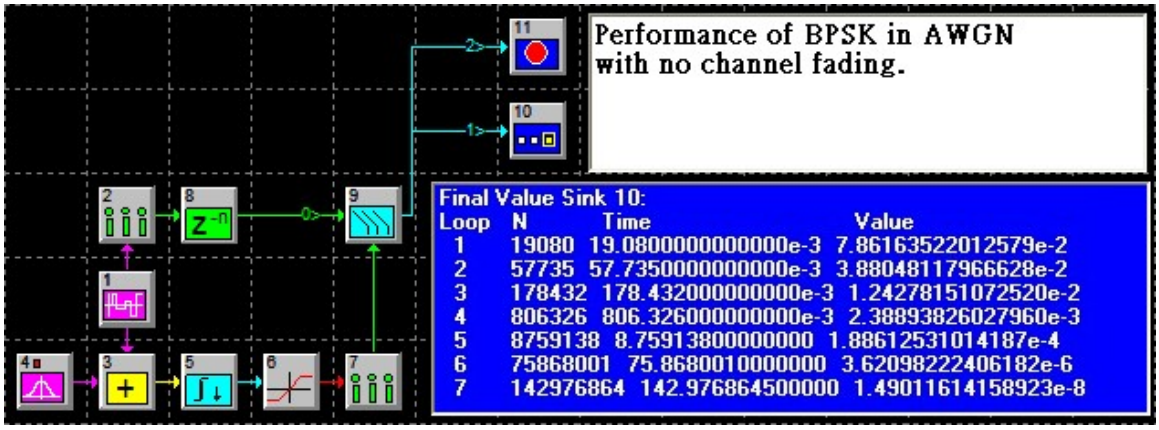


Figure 12. The simulation of baseband BPSK in SystemView.

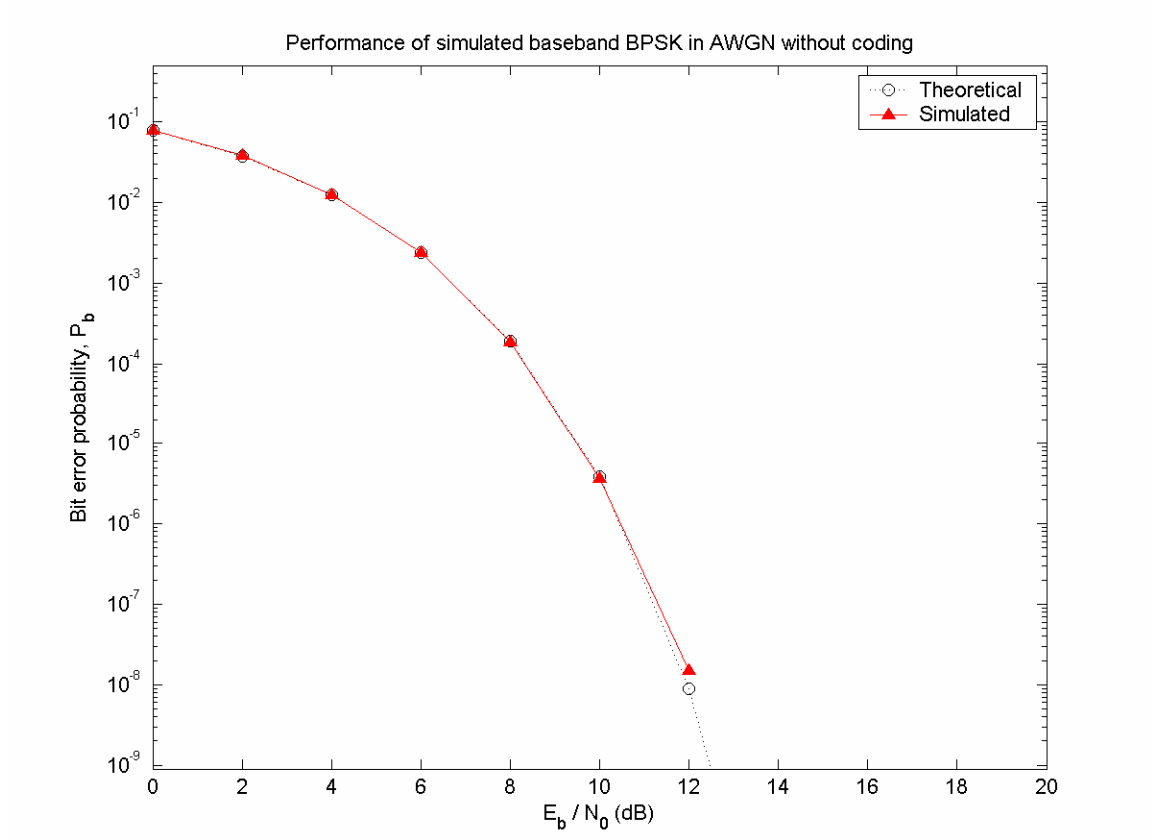


Figure 13. The differences of performance between simulated and theoretical BPSK.

### *b. Simulation of 16QAM in SystemView*

Figures 14 and 15 show the simulation result for 16QAM. Again, there is excellent agreement between the simulation results and the analytical results in equation (4.1).

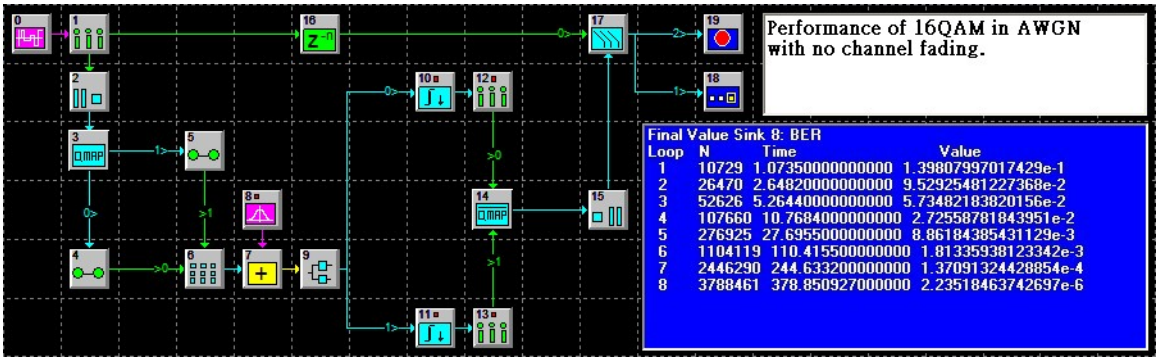


Figure 14. The simulation of 16QAM in SystemView.

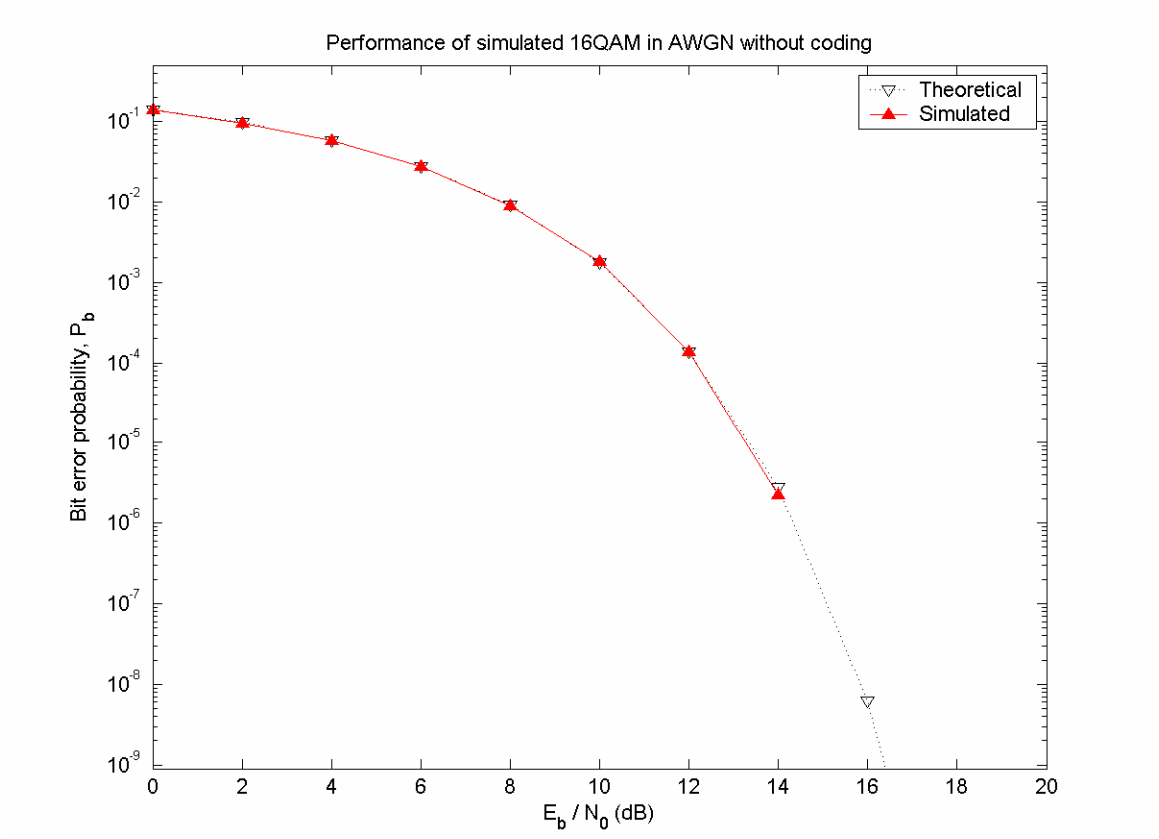


Figure 15. The differences of performance between simulated and theoretical 16QAM.

### *c. Simulation of 16PSK in SystemView*

Figures 16 and 17 show the simulation result for 16PSK which again compare very well with analytical results in equation (4.1).

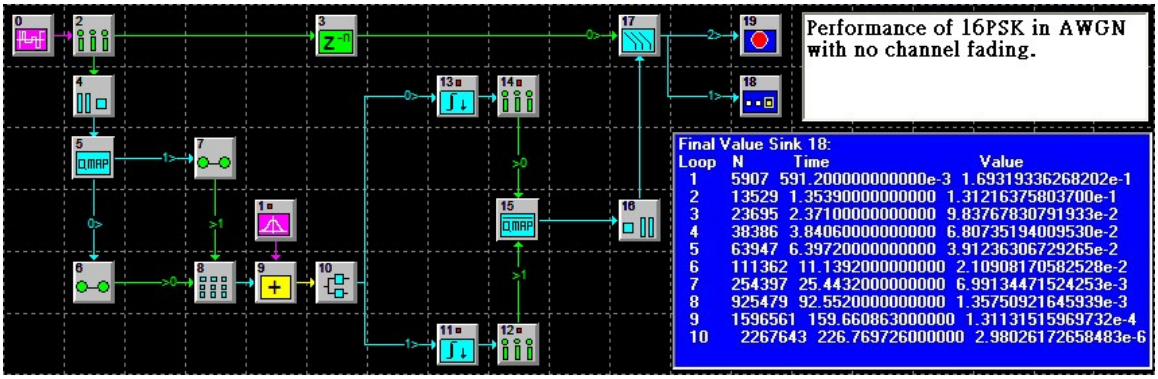


Figure 16. The simulation of 16PSK in SystemView.

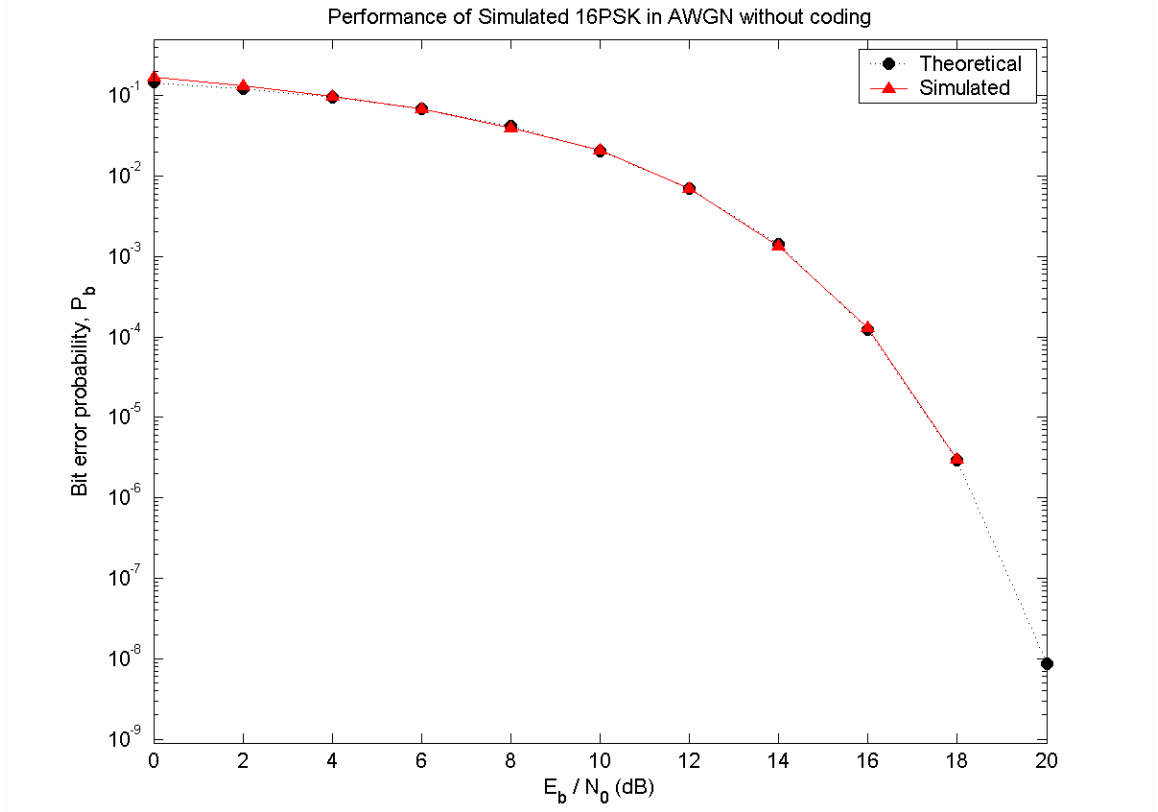


Figure 17. The differences of performance between simulated and theoretical 16PSK.

## B. PERFORMANCE OF COHERENT SYSTEMS WITH CODING

### 1. Convolutional Codes with Hard Decision Decoding

When a code rate $r = k/n$ convolutional code is employed, the probability of bit error is upper bounded by [16]

$$P_b < \frac{1}{k} \sum_{d=d_{free}}^{\infty} B_d P_d \tag{4.2}$$

where $d_{free}$ is the free distance of the convolutional code, $B_d$ is the total number of information bit ones on all weight $d$ code sequences, where $d$ represents the number of code bit one in the sequence, and $P_d$ is the probability of selecting a weight $d$ output sequence as the transmitted code sequence assuming the all zeros sequence was transmitted. The free distance of the convolutional code $d_{free}$ is defined as the weight of the minimum weight of non-zero code sequence. The quantities $B_d$ and $d_{free}$ are parameters of the convolutional code chosen, and $P_d$ is determined by the type of modulation, the channel, and whether hard decision decoding (HDD) or soft decision decoding (SDD) is used. For HDD [16]

$$P_b = \begin{cases} \sum_{i=(d+1)/2}^{d} \binom{d}{i} p^i (1-p)^{d-i} & \text{for } d \text{ odd} \\ \frac{1}{2}\binom{d}{d/2}[p(1-p)]^{d/2} + \sum_{i=1+d/2}^{d} \binom{d}{i} p^i (1-p)^{d-i} & \text{for } d \text{ even} \end{cases} \tag{4.3}$$

where $p$ is the probability of channel bit error.

The free distances and the first eight $B_d$s of commonly used $r = 1/2$ convolutional codes are listed in Table 2 [9], and the corresponding generator polynomials are listed in Table 3 [17]. The generator polynomials are a concise way of specifying the connections from convolutional encoder shift register input and output to the coded outputs. For example, the generator polynomials (131,171) (expressed in octal) define the $r = 1/2$ convolutional encoder shown in Figure 18. [18]

Table 2. Best (maximum free distance) rate 1/2, convolutional code information weight structure (From Ref. 9)

| $\nu$ | $d_{free}$ | $B_{d_{free}}$ | $B_{d_{free}+1}$ | $B_{d_{free}+2}$ | $B_{d_{free}+3}$ | $B_{d_{free}+4}$ | $B_{d_{free}+5}$ | $B_{d_{free}+6}$ | $B_{d_{free}+7}$ |
|---|---|---|---|---|---|---|---|---|---|
| 3 | 5 | 1 | 4 | 12 | 32 | 80 | 192 | 448 | 1024 |
| 4 | 6 | 2 | 7 | 18 | 49 | 130 | 333 | 836 | 2069 |
| 5 | 7 | 4 | 12 | 20 | 72 | 225 | 500 | 1324 | 3680 |
| 6 | 8 | 2 | 36 | 32 | 62 | 332 | 701 | 2342 | 5503 |
| 7 | 10 | 36 | 0 | 211 | 0 | 1404 | 0 | 11633 | 0 |
| 8 | 10 | 2 | 22 | 60 | 148 | 340 | 1008 | 2642 | 6748 |
| 9 | 12 | 33 | 0 | 281 | 0 | 2179 | 0 | 15035 | 0 |

Table 3. Best (maximum free distance) rate 1/2, convolutional code generators (in octal) (From Ref. 17).

| $\nu$ | Generators | $d_{free}$ | $B_{d_{free}}$ | $B_{d_{free}+5}$ | $B_{d_{free}+6}$ | $B_{d_{free}+7}$ |
|---|---|---|---|---|---|---|
| 3 | 7,5 | 5 | 1 | 192 | 448 | 1024 |
| 4 | 17,15 | 6 | 2 | 333 | 836 | 2069 |
| 5 | 35,23 | 7 | 4 | 500 | 1324 | 3680 |
| 6 | 75,53 | 8 | 2 | 701 | 2342 | 5503 |
| 7 | 171,133 | 10 | 36 | 0 | 11633 | 0 |
| 8 | 371,247 | 10 | 2 | 1008 | 2642 | 6748 |
| 9 | 753,561 | 12 | 33 | 0 | 15035 | 0 |

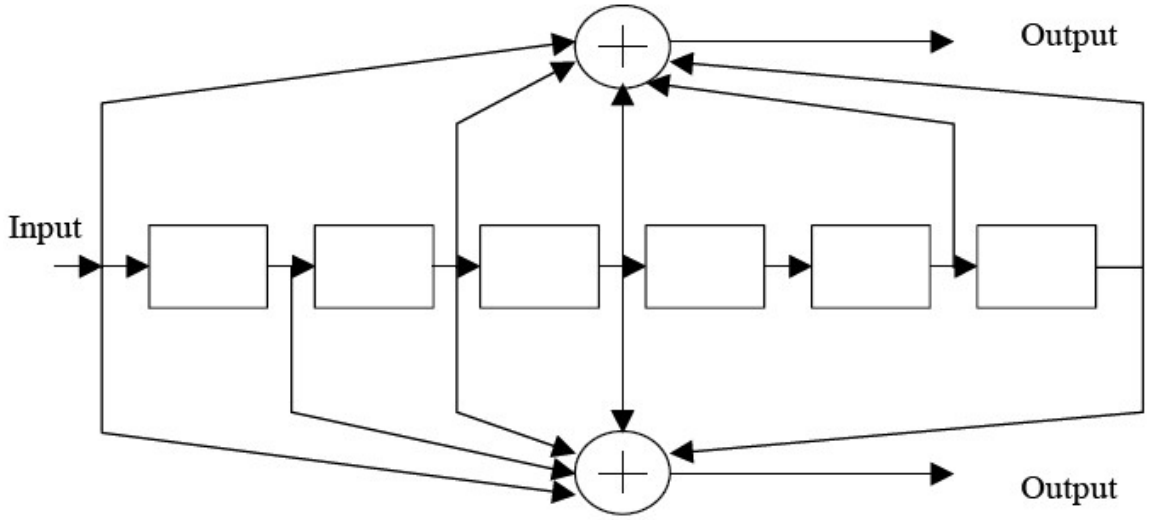


Figure 18. The $r = 1/2$, constraint length 7 convolutional encoder defined by the generator polynomials (131,171). (From Ref. 18)

### 2. Simulation of Convolutional Coded BPSK with Hard Decision Decoding

Figures 19 and 20 show the simulation results for BPSK in AWGN with $r = 1/2$, $\nu = 3$ convolutional source coding and HDD, which compare well with the analytical upper bound in equation (4.2) for higher SNR.

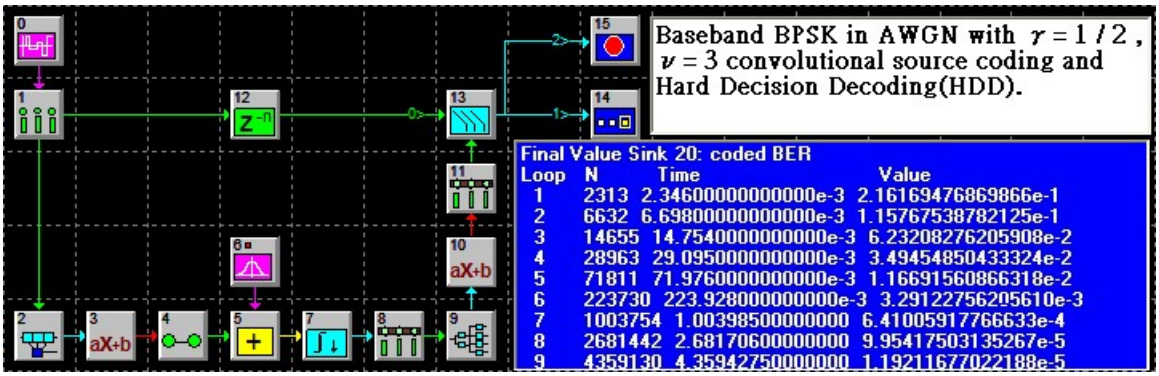


Figure 19. The simulation of baseband BPSK in AWGN with $r = 1/2$ , $\nu = 3$ convolutional source coding and HDD.

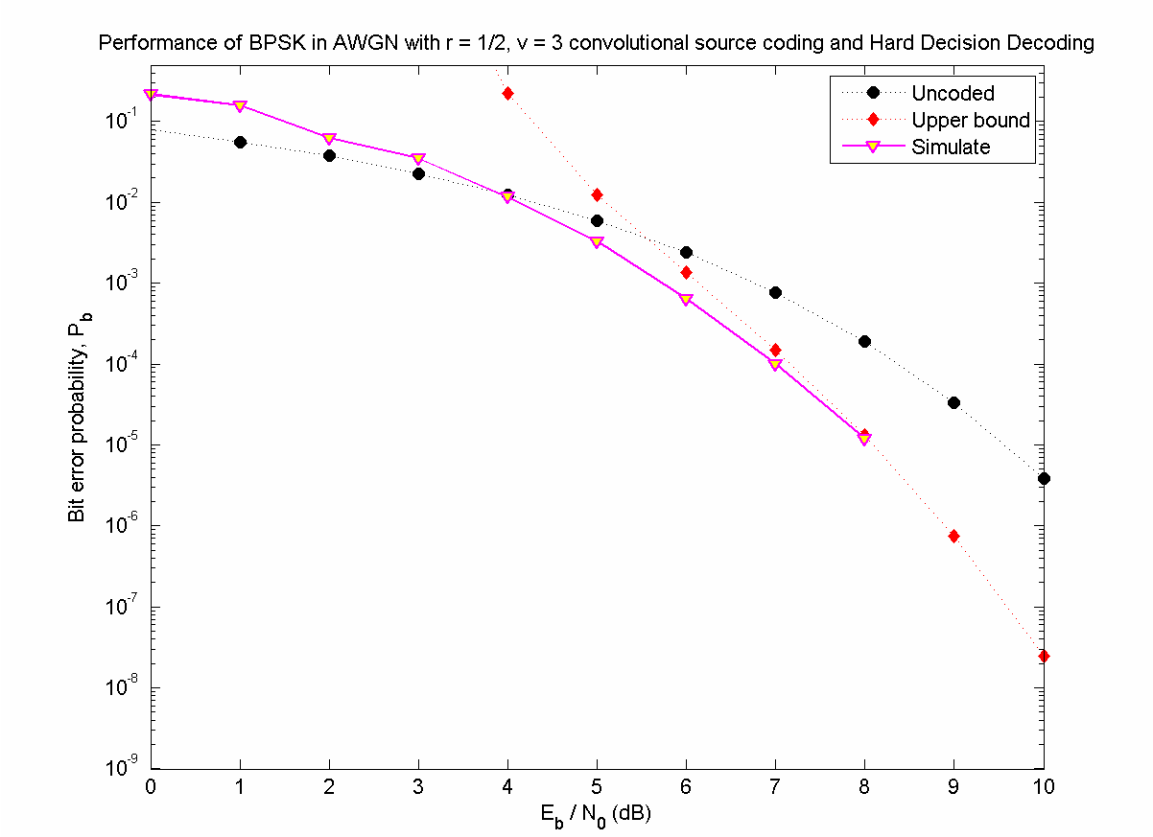


Figure 20. Performance for BPSK with $r = 1/2$ , $\nu = 3$ convolutional source coding and HDD.

### 3. Simulation of Convolutional Coded BPSK with Hard Decision Decoding and Barrage Noise Jamming

The primary motivation for simulating communication systems is to provide an evaluation tool for systems that are difficult to analyze. In this subsection, this principle is illustrated by using the example of BPSK with $r = 1/2$ , $\nu = 3$ convolutional coding where the signal is affected by barrage noise as well as AWGN. Since the barrage noise is just more AWGN, we expect the BER performance for cases where $E_b / N_I << E_b / N_0$ to be approximately the sum as for the corresponding $E_b / N_0$ in the AWGN only case, as illustrated in Figure 20. The simulation results for $E_b / N_0 = 13.35$ dB and HDD are shown in Figures 21 and 22 and correspond well with what is expected when $E_b / N_I << E_b / N_0$ .

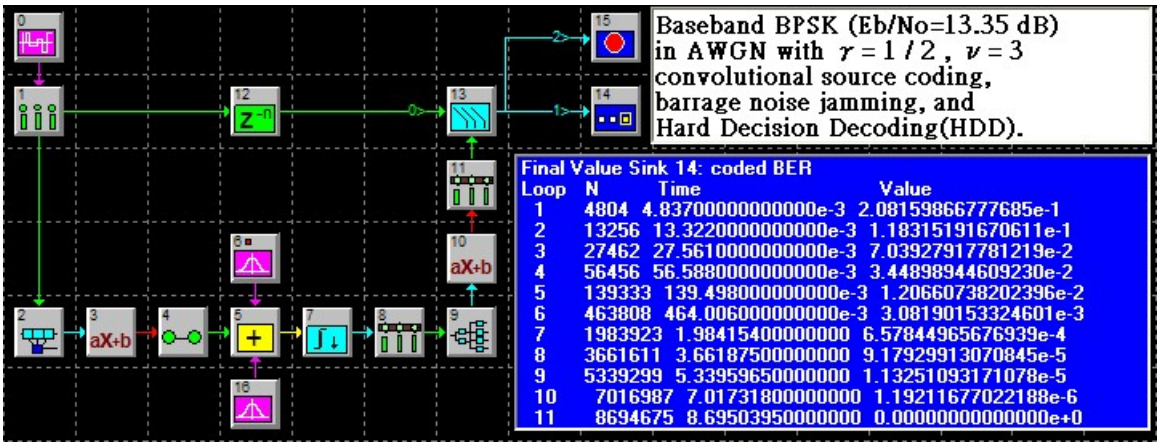


Figure 21. The simulation of baseband BPSK in AWGN with $r = 1/2$ , $\nu = 3$ convolutional source coding, HDD, and barrage noise jamming.

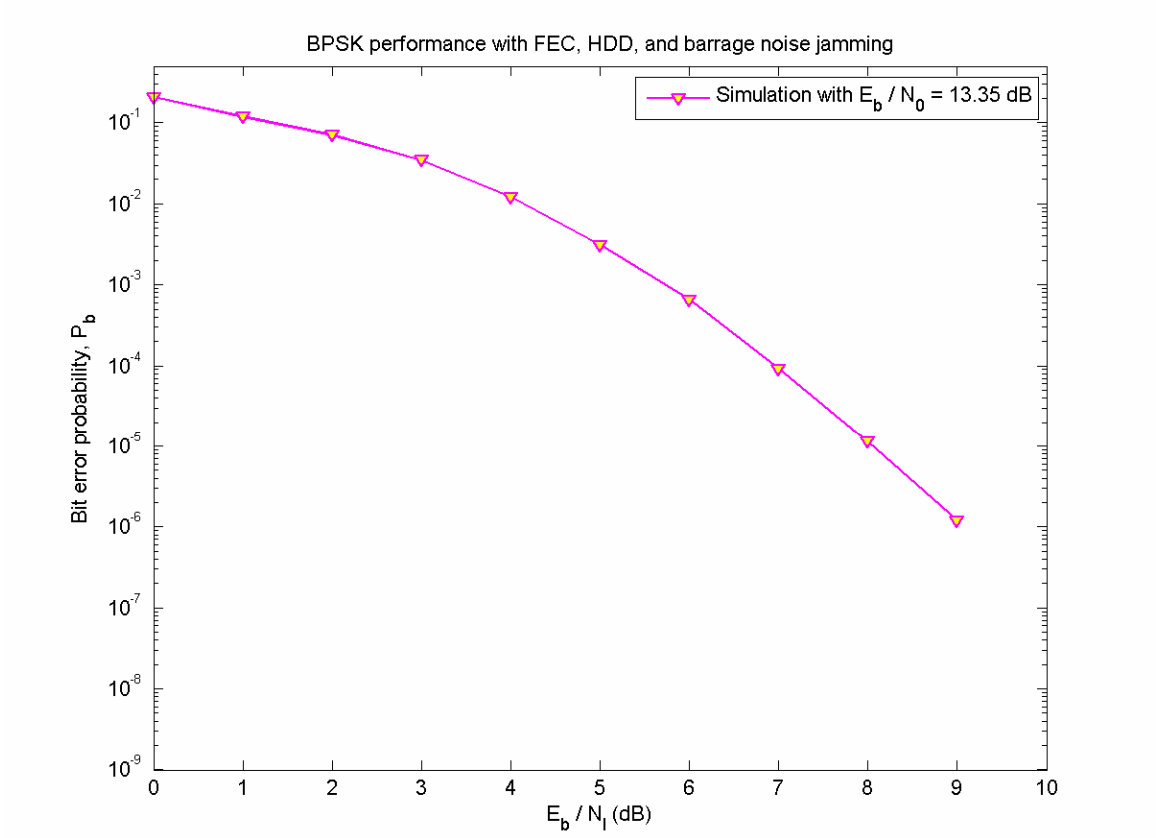


Figure 22. Performance for BPSK with $r = 1/2$ , $\nu = 3$ convolutional source coding, HDD, and barrage noise jamming.

## 4. Convolutional Codes with Soft Decision Decoding

For soft decision detection with BPSK, we assume that the receiver is a maximal ratio combiner.[7] The probability of bit error for BPSK in AWGN with rate $r = 1/2$ convolutional source coding and soft decision decoding is of the form [15]

$$P_d = \frac{1}{2\sqrt{\pi rc}}\left[\frac{2(1+\zeta)}{2(1+\zeta)+br\overline{\gamma_b}}\right]^d \exp\left[\frac{-brd\zeta\overline{\gamma_b}}{2(1+\zeta)+br\overline{\gamma_b}}\right] \tag{4.4}$$

where b is given in Table 1, $c = 1.0 + 0.1\zeta$ is empirically obtained, $\zeta$ is the Ricean factor, and $\overline{\gamma_b}$ is the average $E_b / N_0$.

## 5. Simulation of Convolutional Coded BPSK with Soft Decision Decoding

Figures 23 and 24 show the simulation results for BPSK in AWGN with $r = 1/2$, $\nu = 3$ convolutional source coding and SDD, which compare well with the analytical upper bound in equation (4.2) for high SNR. For $E_b / N_0 > 6$ dB, simulation results were not obtained due to the excessive runtime required.

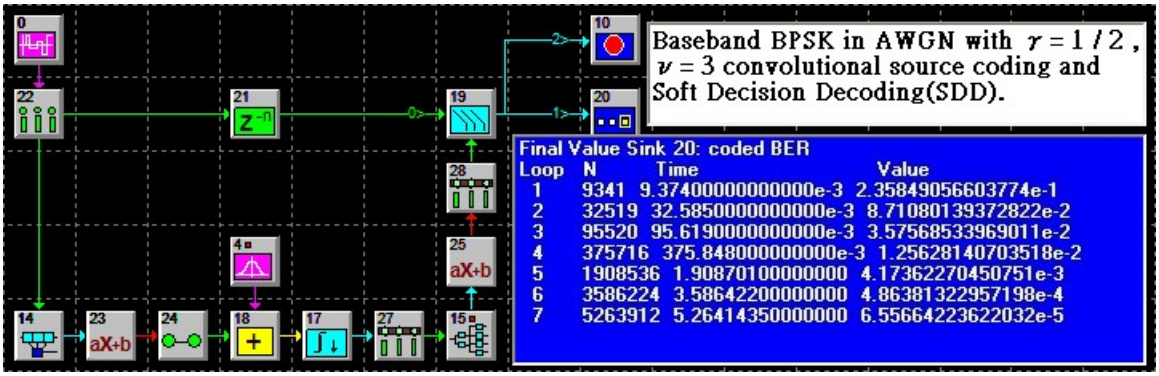


Figure 23. The simulation of baseband BPSK in AWGN with $r = 1/2$, $\nu = 3$ convolutional source coding and SDD.

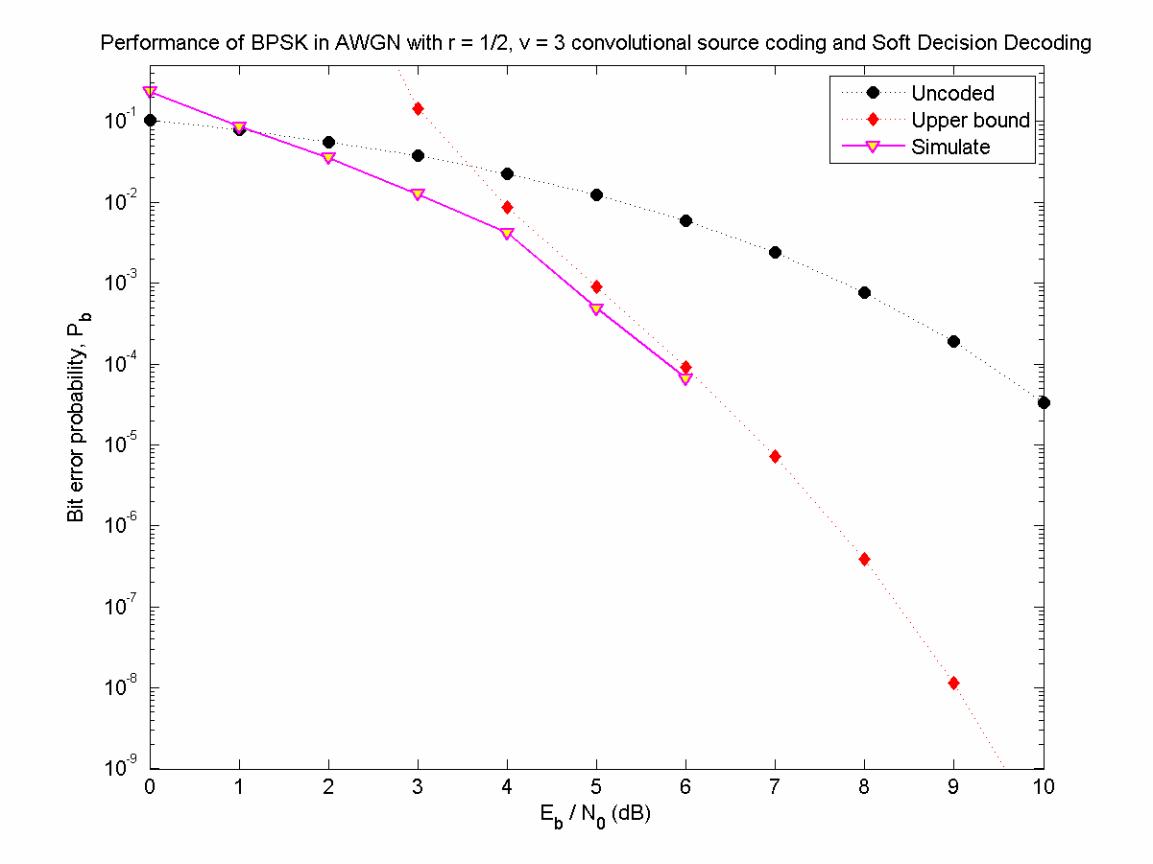


Figure 24. Performance for BPSK with $r = 1/2$ , $\nu = 3$ convolutional source coding and SDD.

### 6. Simulation of Convolutional Coded BPSK with Soft Decision Decoding, and Barrage Noise Jamming

Analogous to section IV.B.3, in this subsection the effect of both barrage noise and AWGN on a system utilizing BPSK with $r = 1/2$ , $\nu = 3$ convolutional coding is simulated, only here SDD is used. As with HDD, simulation results are obtained for $E_b / N_0 = 13.35$ dB. We except the BER performance for cases where $E_b / N_I << E_b / N_0$ to be approximately the sum as for the corresponding $E_b / N_0$ in the AWGN only case, as illustrated in Figure 24. The results are shown in Figures 25 and 26 and, as with HDD, correspond well with what is expected when $E_b / N_0 >> E_b / N_I$ .

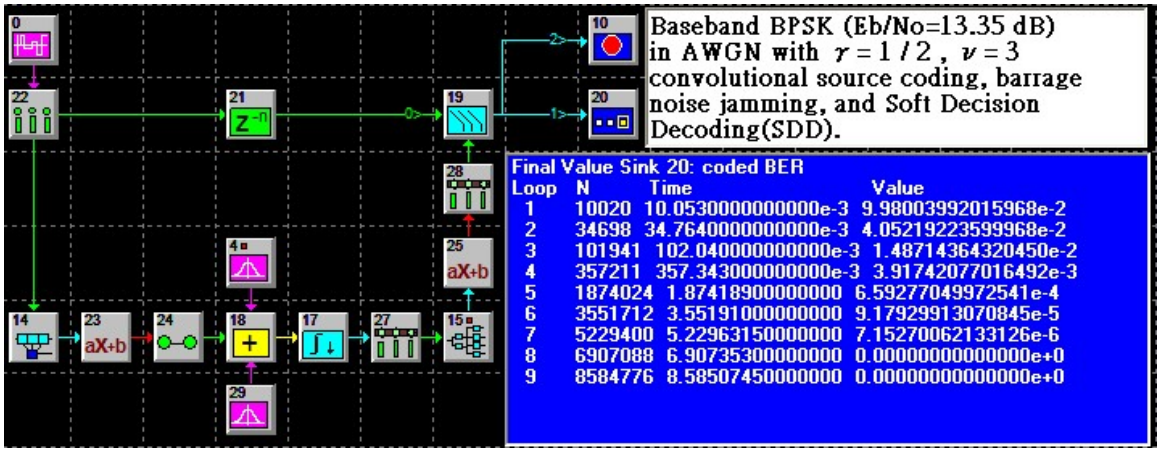


Figure 25. The simulation of baseband BPSK in AWGN with $r = 1/2$ , $\nu = 3$ convolutional source coding, SDD, and barrage noise jamming.

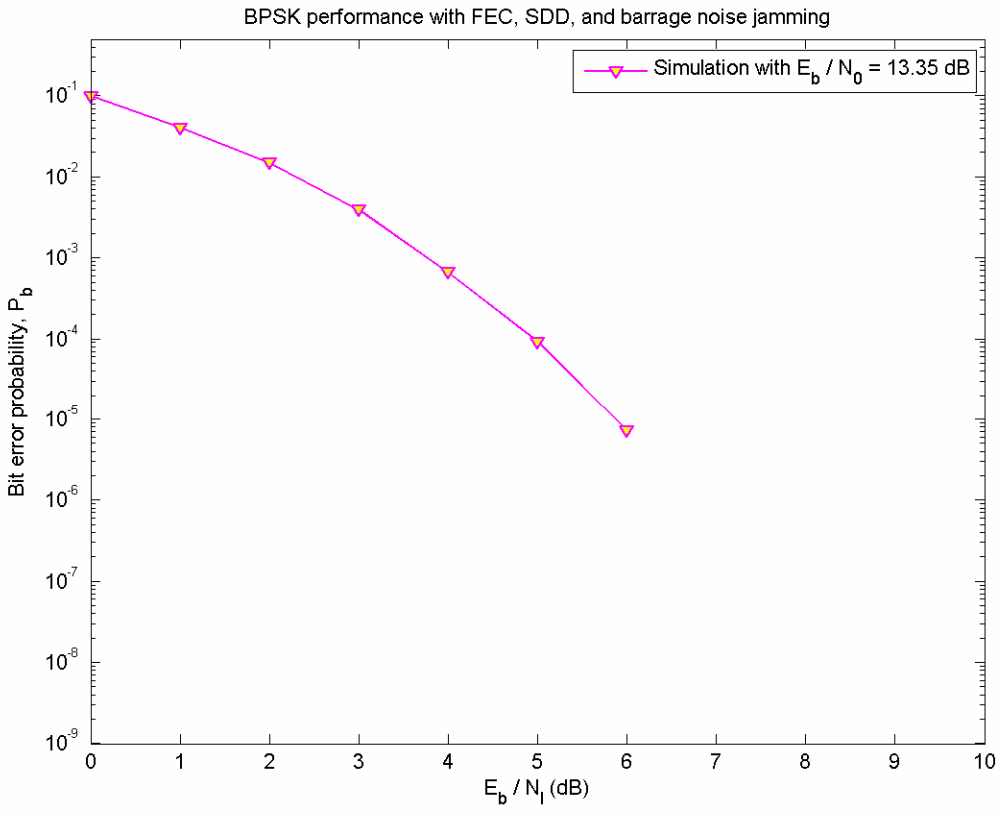


Figure 26. Performance for BPSK with $r = 1/2$ , $\nu = 3$ convolutional source coding, SDD, and barrage noise jamming.

## C. FADING CHANNELS

### 1. Performance of Coherent System with Flat, Slow Fading Channels

For BPSK received through a flat, slow, Rayleigh fading channel, the bit error ratio (BER) is, [15]

$$P_b = \frac{1}{2}\left(1 - \sqrt{\frac{\overline{\gamma_b}}{1+\overline{\gamma_b}}}\right) \tag{4.5}$$

and $\overline{\gamma_b}$ is the average $E_b / N_0$.

For *M*PSK and Rayleigh fading, the BER is, [15]

$$P_b = \frac{1}{q}\left(1 - \sqrt{\frac{q\overline{\gamma_b}\sin^2(\pi/M)}{1+q\overline{\gamma_b}\sin^2(\pi/M)}}\right) \tag{4.6}$$

For *M*QAM with $q$ even and Rayleigh fading, the BER is, [15]

$$P_b = \frac{2}{q}(1-2^{-q/2})\left(1 - \sqrt{\frac{3q\overline{\gamma_b}}{2(2^q-1)+3q\overline{\gamma_b}}}\right) \tag{4.7}$$

For *M*QAM with $q$ odd $(q \geq 3)$ and Rayleigh fading, the BER is, [15]

$$P_b = \frac{2}{q}\left(1 - \sqrt{\frac{3q\overline{\gamma_b}}{2(2^q-1)+3q\overline{\gamma_b}}}\right) \tag{4.8}$$

For BPSK and Ricean fading, the BER is, [15]

$$P_b \approx \frac{1}{2\sqrt{\pi c}}\left(\frac{\zeta+1}{\overline{\gamma_b}+\zeta+1}\right)\exp\left(\frac{-\zeta\overline{\gamma_b}}{\overline{\gamma_b}+\zeta+1}\right) \tag{4.9}$$

where $c = 1.2 + 0.1\zeta$ is empirically obtained.

For *M*PSK and Ricean fading, the BER is, [15]

$$P_b = \frac{1+\zeta}{q\sqrt{\pi c}[1+\zeta+q\sin^2(\pi/M)\overline{\gamma_b}]}\exp\left(\frac{-q\sin^2(\pi/M)\zeta\overline{\gamma_b}}{1+\zeta+q\sin^2(\pi/M)\overline{\gamma_b}}\right) \tag{4.10}$$

where $c$ is empirically obtained.

For *M*QAM with $q$ even and Ricean fading, the BER is, [15]

$$P_b \approx \frac{4(1-1/2^{q/2})(2^q-1)(\zeta+1)}{q\sqrt{\pi c}[3q\overline{\gamma_b}+2(2^q-1)(\zeta+1)]}\exp\left(\frac{-3q\zeta\overline{\gamma_b}}{3q\overline{\gamma_b}+2(2^q-1)(\zeta+1)}\right) \tag{4.11}$$

where $c = 1.3 + 0.05\zeta$ is empirically obtained.

For *M*QAM with $q$ odd and Ricean fading, the BER is, [15]

$$P_b \approx \frac{4(1-1/2^{q/2})(\zeta+1)}{q\sqrt{\pi c}[3q\overline{\gamma_b}+2(2^q-1)(\zeta+1)]}\exp\left(\frac{-3q\zeta\overline{\gamma_b}}{3q\overline{\gamma_b}+2(2^q-1)(\zeta+1)}\right) \tag{4.12}$$

where $c = 1.3 + 0.05\zeta$ is empirically obtained.

## 2. Simulation of Coherent Systems in SystemView with Fading Channels

### *a. Rayleigh Fading*

(1) BPSK. The performance of baseband BPSK transmitted over a slow, flat Rayleigh fading channel is shown in Figures 27 and 28. The results of the analytical expression in equation (4.5) are also shown in Figure 28 and shows excellent agreement with the simulated results.

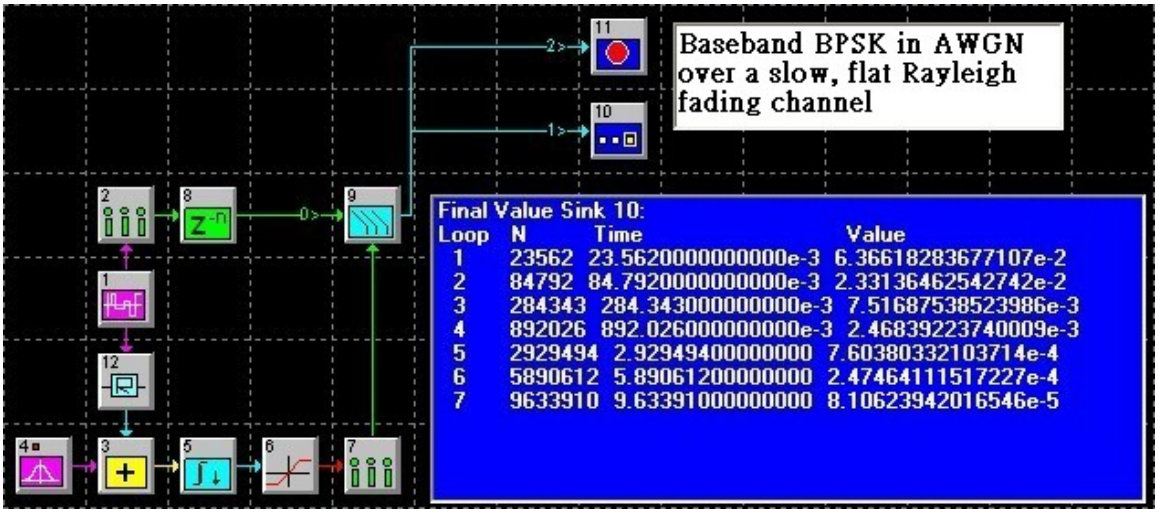


Figure 27. Baseband BPSK in AWGN over a slow, flat Rayleigh fading channel.

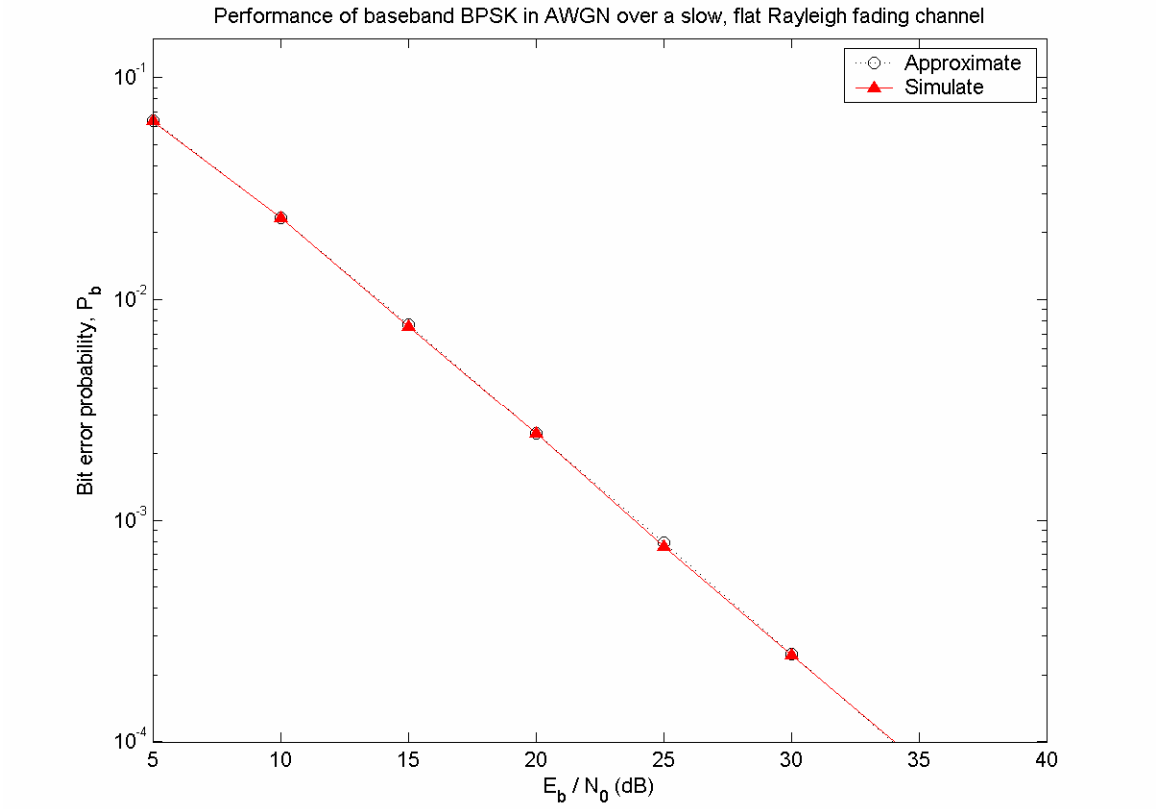


Figure 28. The performance for simulated and approximate baseband BPSK in AWGN over a slow, flat Rayleigh fading channel.

(2) 16QAM. Figures 29 and 30 show the simulation results for 16QAM in AWGN over a slow, flat Rayleigh fading channel. There is excellent agreement between the simulation results and the analytical results in equation (4.7).

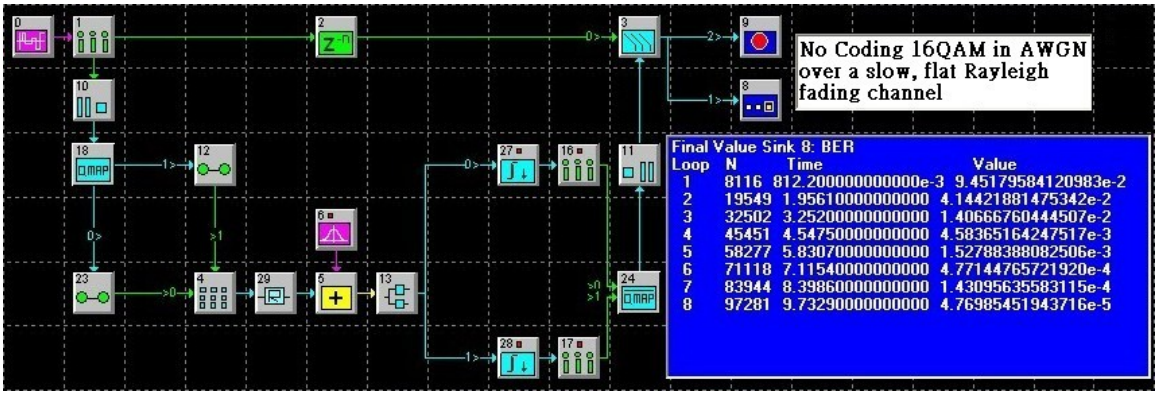


Figure 29. 16QAM in AWGN over a slow, flat Rayleigh fading channel.

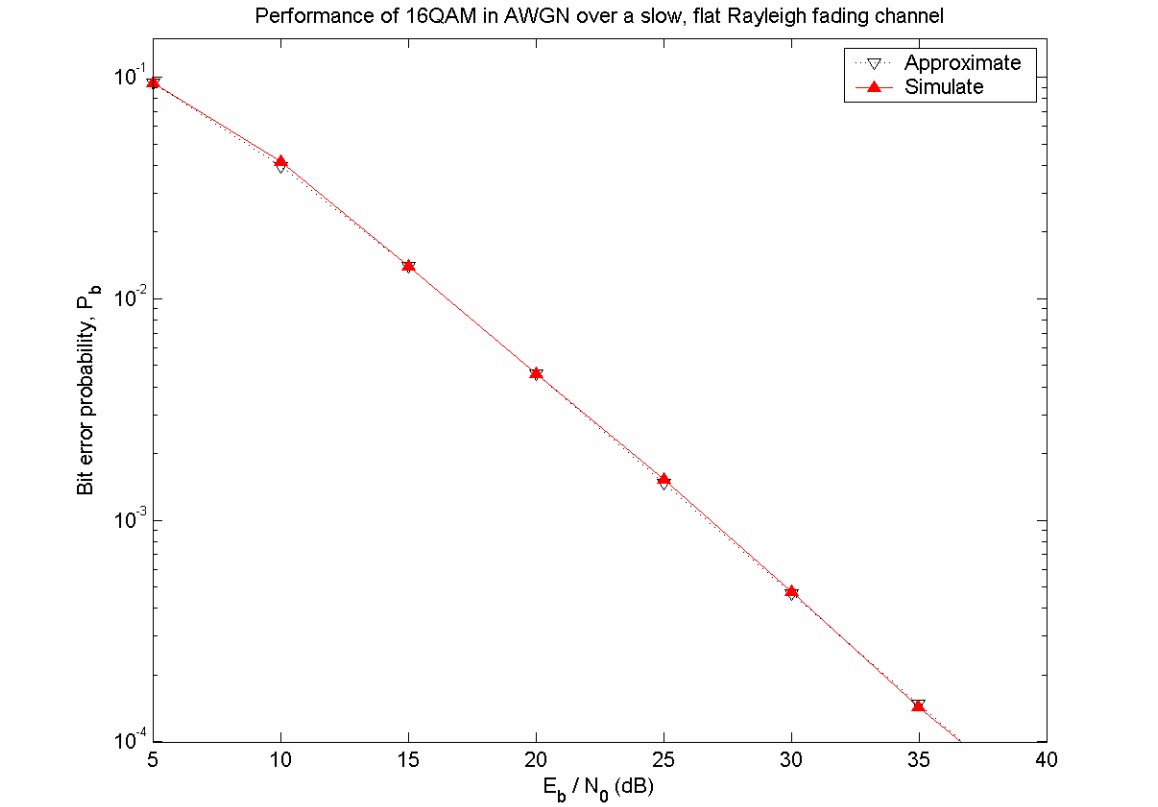


Figure 30. The performance for simulated and approximate 16QAM in AWGN over a slow, flat Rayleigh fading channel.

(3) 16PSK. Figures 31 and 32 show the simulation results for 16PSK in AWGN over a slow, flat Rayleigh fading channel. There is good agreement between the simulation results and the analytical results in equation (4.6).

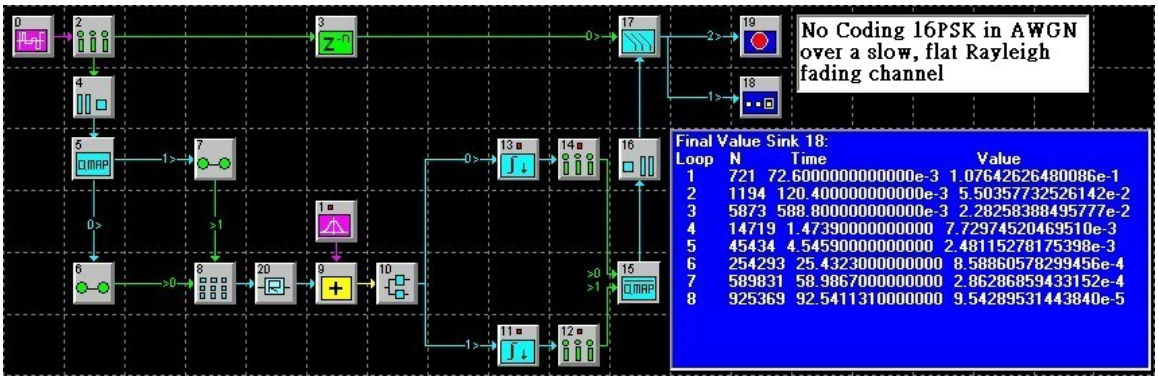


Figure 31. 16PSK in AWGN over a slow, flat Rayleigh fading channel.

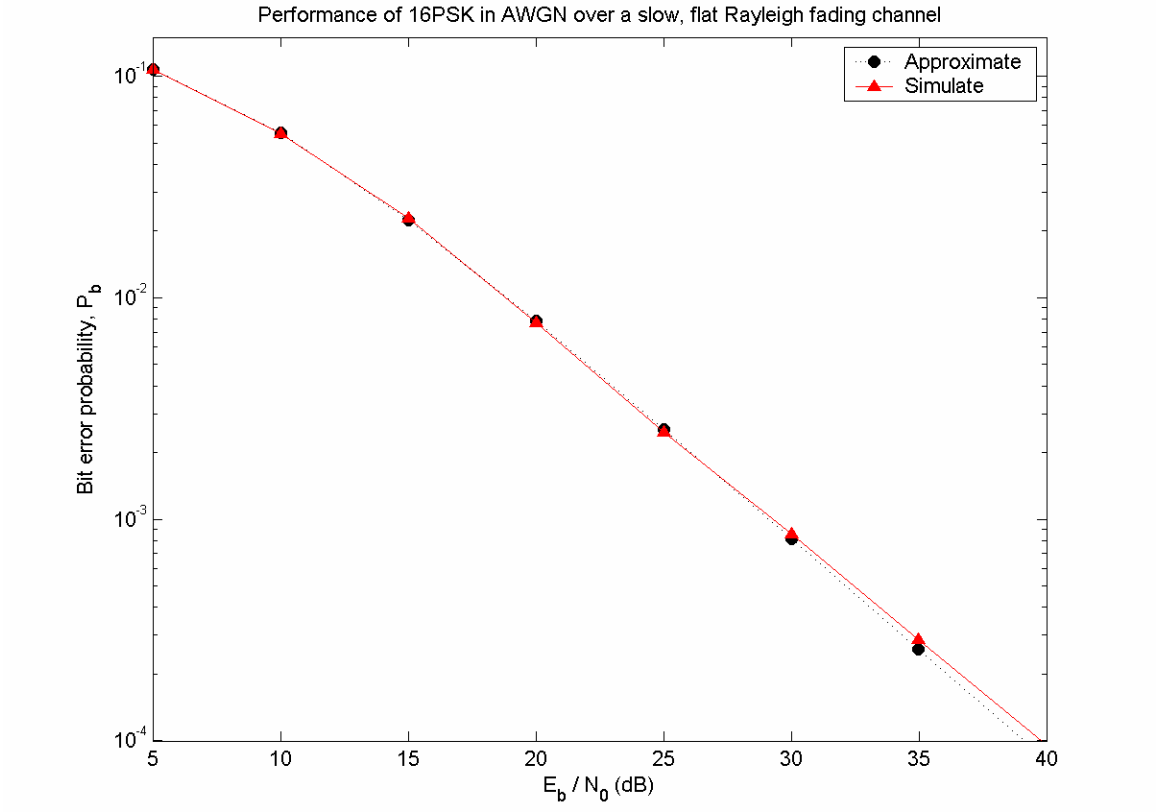


Figure 32. The performance for simulated and approximate 16PSK in AWGN over a slow, flat Rayleigh fading channel.

### *b. Ricean Fading, $\zeta = 4$*

(1) BPSK. Figures 33 and 34 show the simulation results for baseband BPSK in AWGN over a slow, flat Ricean fading channel with $\zeta = 4$. There is good agreement between the simulation results and the analytical results in equation (4.9).

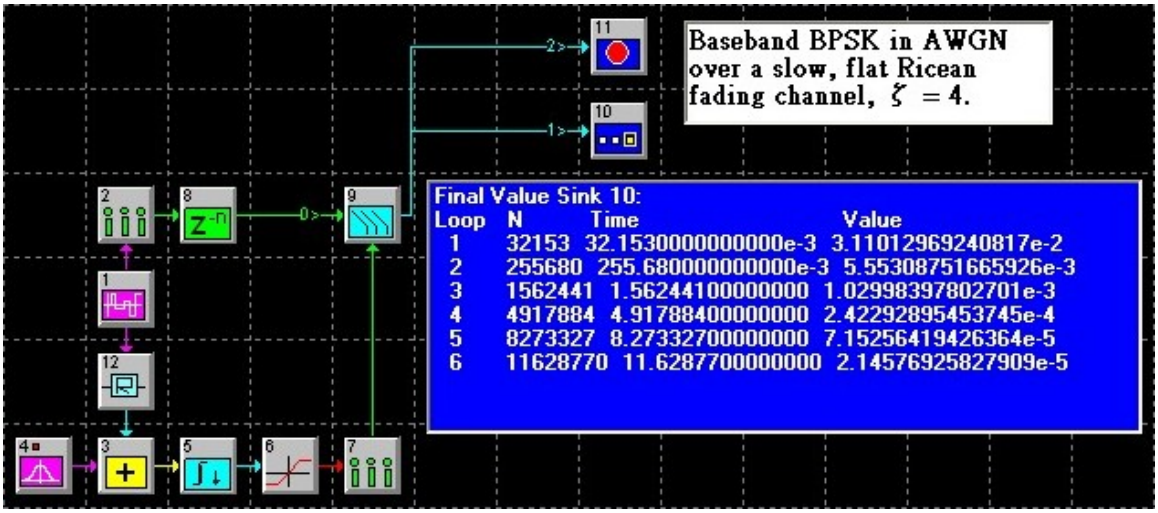


Figure 33. Baseband BPSK in AWGN over a slow, flat Ricean fading channel with $\zeta = 4$.

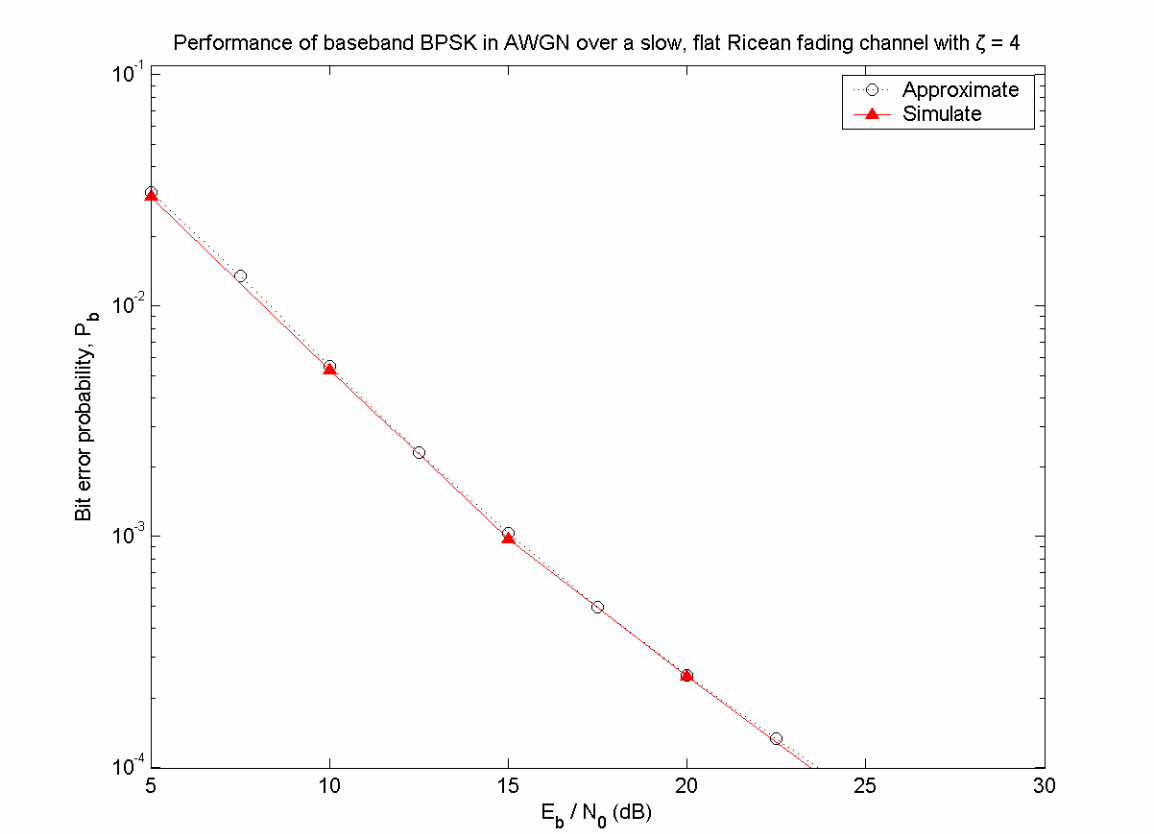


Figure 34. The performance for simulated and approximate Baseband BPSK in AWGN over a slow, flat Ricean fading channel with $\zeta = 4$.

(2) 16QAM. Figures 35 and 36 show the simulation results for 16QAM in AWGN over a slow, flat Ricean fading channel with $\zeta = 4$. There is excellent agreement between the simulation results and the analytical results in equation (4.11).

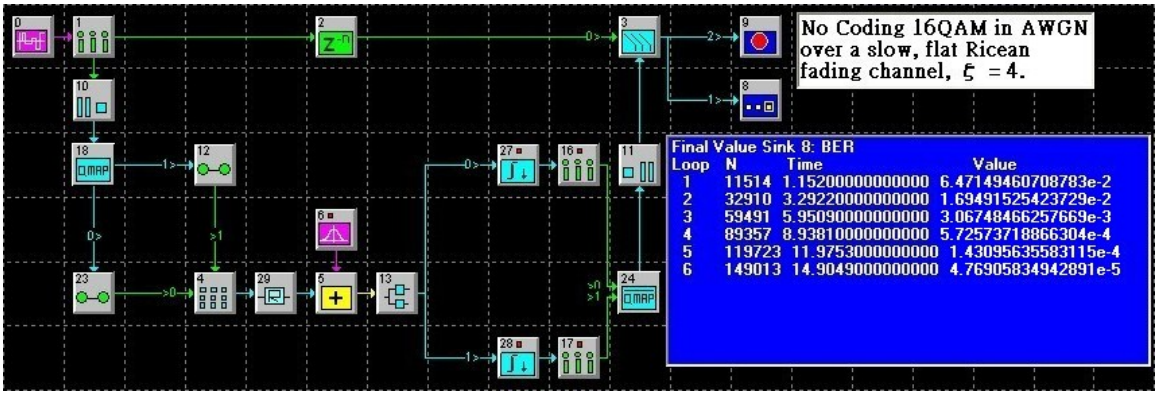


Figure 35. 16QAM in AWGN over a slow, flat Ricean fading channel with $\zeta = 4$.

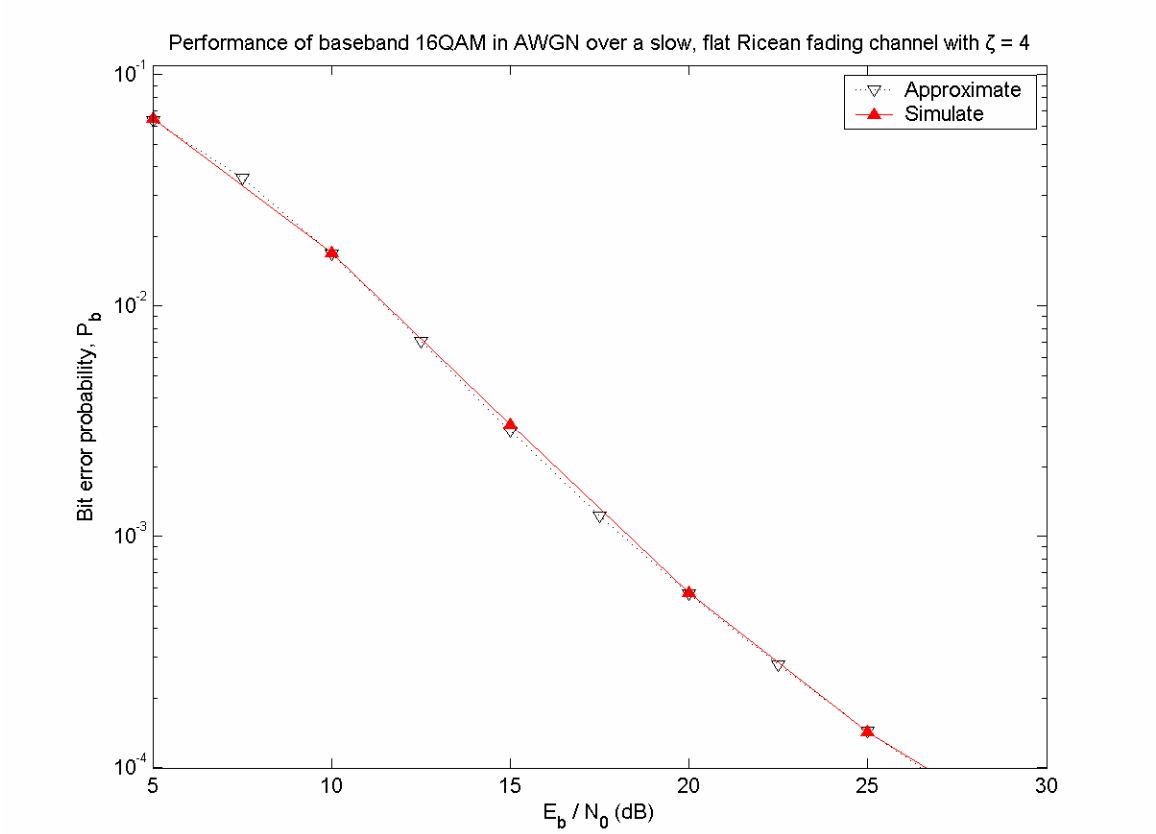


Figure 36. The performance for simulated and approximate 16QAM in AWGN over a slow, flat Ricean fading channel with $\zeta = 4$.

(3) 16PSK. Figures 37 and 38 show the simulation results for 16PSK in AWGN over a slow, flat Ricean fading channel with $\zeta = 4$. There is very good agreement between the simulation results and the analytical results in equation (4.10).

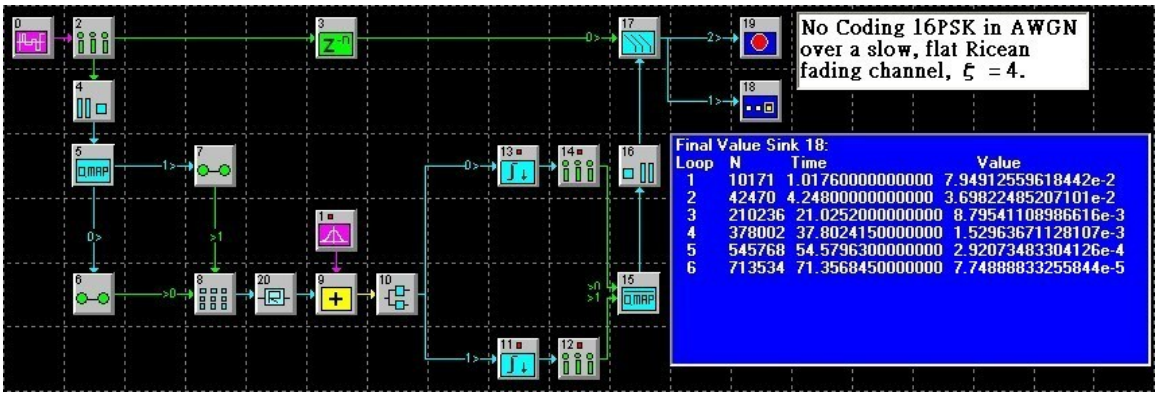


Figure 37. 16PSK in AWGN over a slow, flat Ricean fading channel with $\zeta = 4$.

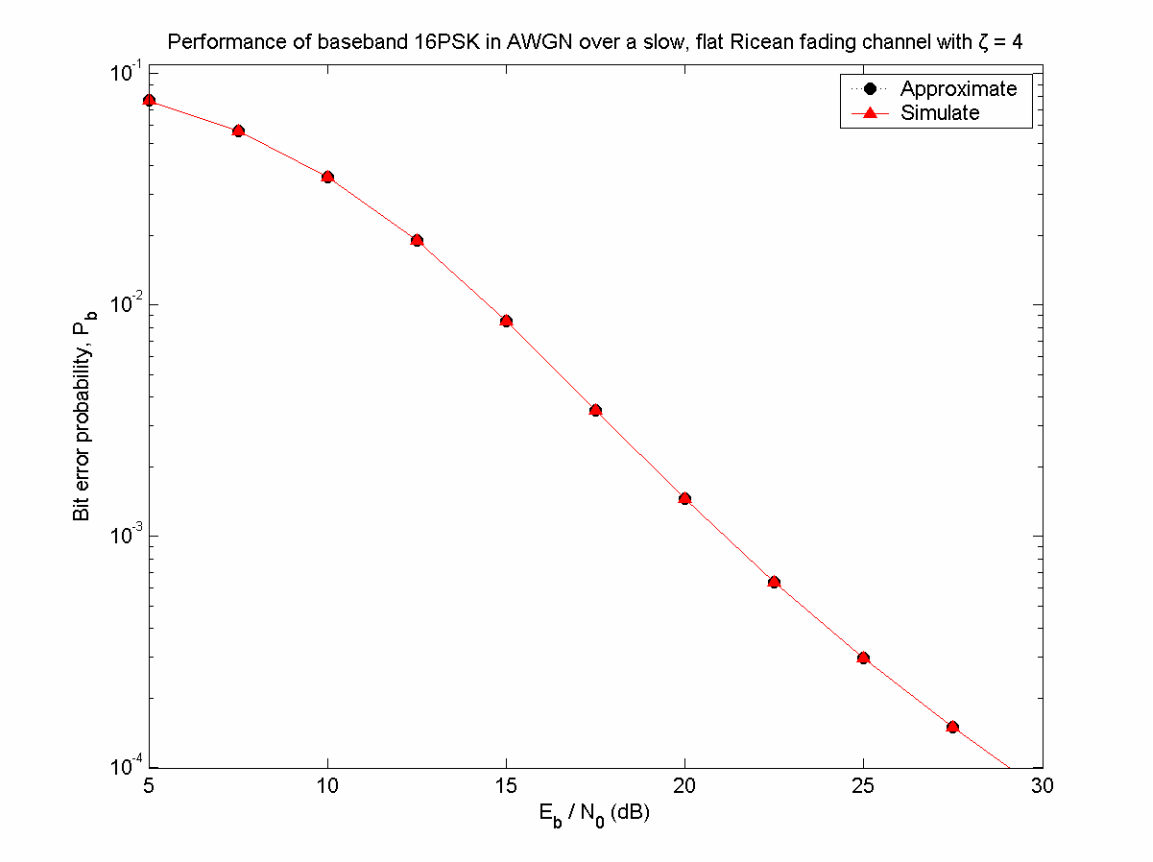


Figure 38. The performance for simulated and approximate 16PSK in AWGN over a slow, flat Ricean fading channel with $\zeta = 4$.

***c. Ricean Fading,*** $\zeta = 10$

(1) BPSK. Figures 39 and 40 display the simulation results for baseband BPSK in AWGN over a slow, flat Ricean fading channel with $\zeta = 10$. There is good agreement between the simulation results and the analytical results.

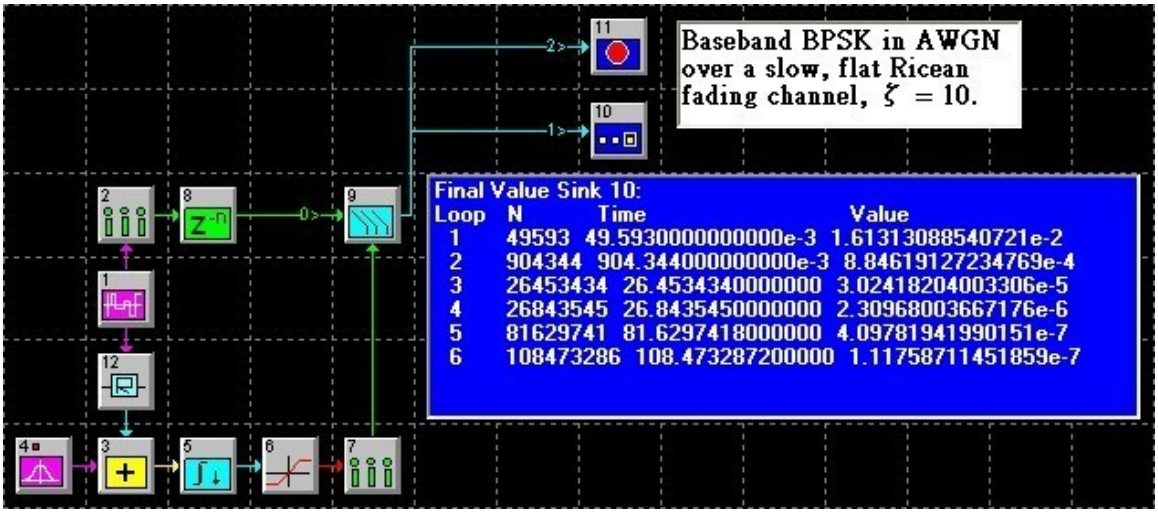


Figure 39. Baseband BPSK in AWGN over a slow, flat Ricean fading channel with $\zeta = 10$.

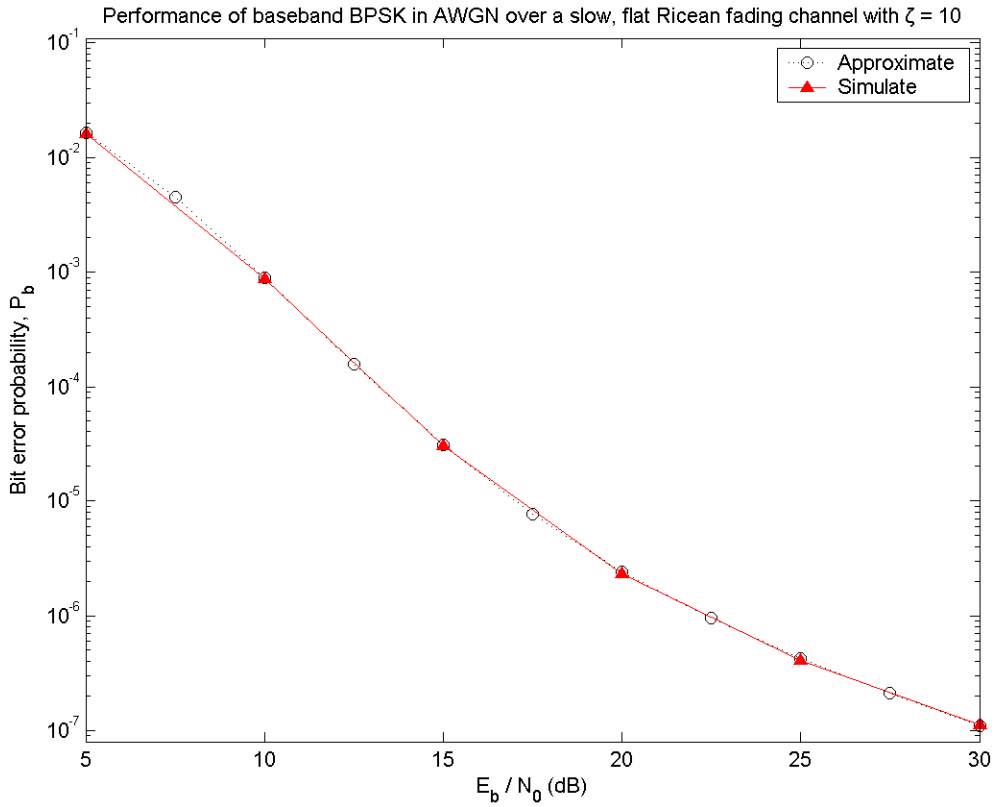


Figure 40. The performance for simulated and approximate Baseband BPSK in AWGN over a slow, flat Ricean fading channel with $\zeta = 10$.

(2) 16QAM. Figures 41 and 42 display the simulation results for 16QAM in AWGN over a slow, flat Ricean fading channel with $\zeta = 10$. There is good agreement between the simulation results and the analytical results.

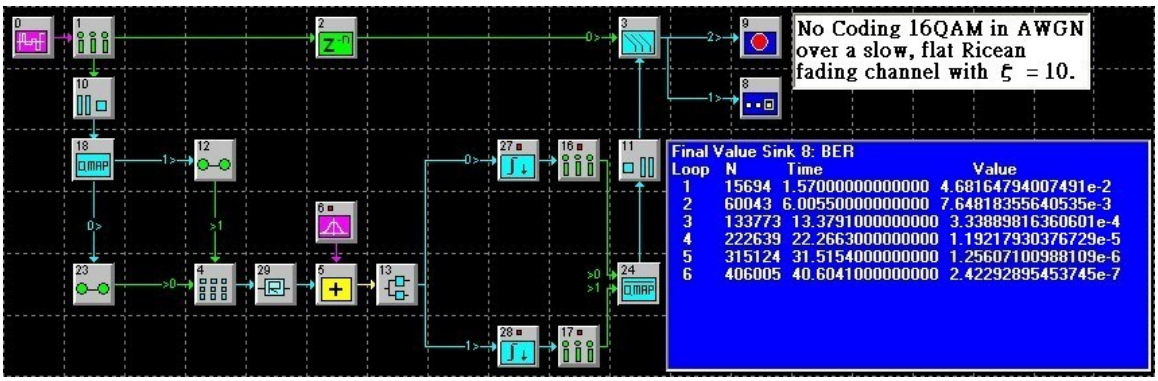


Figure 41. 16QAM in AWGN over a slow, flat Ricean fading channel with $\zeta = 10$.

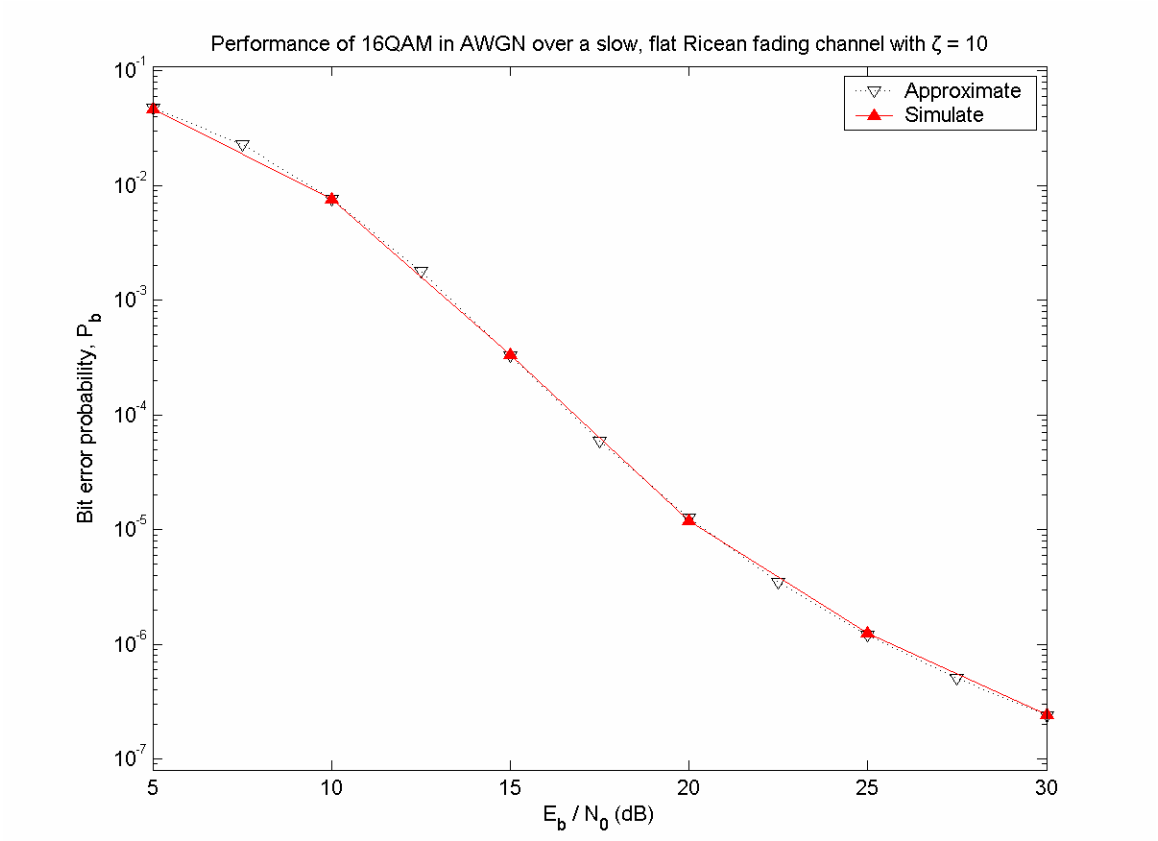


Figure 42. The performance for simulated and approximate 16QAM in AWGN over a slow, flat Ricean fading channel with $\zeta = 10$.

(3) 16PSK. Figures 43 and 44 display the simulation results for 16PSK in AWGN over a slow, flat Ricean fading channel with $\zeta = 10$. There is a good agreement between the simulation results and the analytical results.

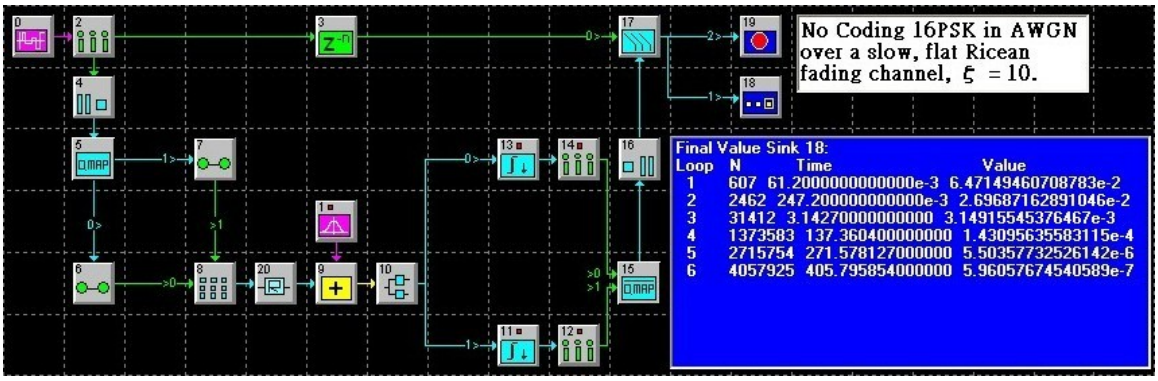


Figure 43. 16PSK in AWGN over a slow, flat Ricean fading channel with $\zeta = 10$.

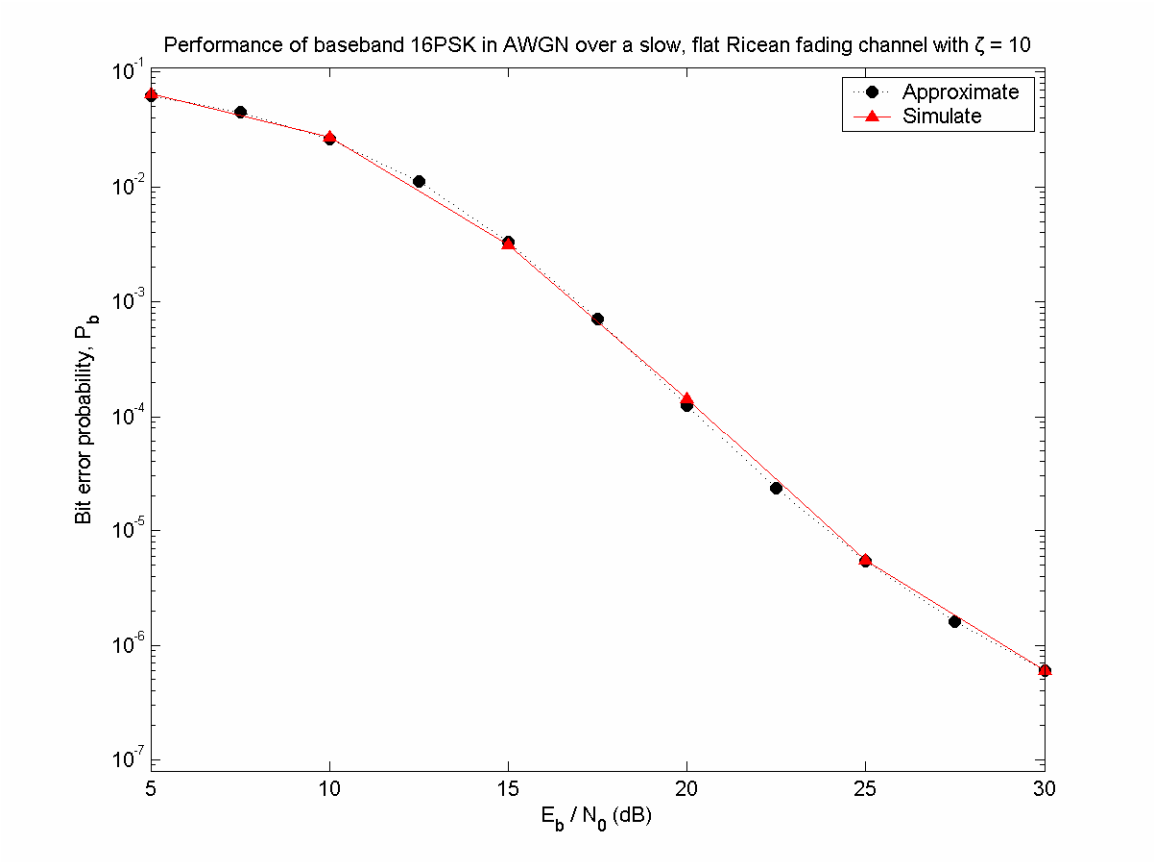


Figure 44. The performance for simulated and approximate 16PSK in AWGN over a slow, flat Ricean fading channel with $\zeta = 10$.

## C. CHAPTER SUMMARY

In this chapter, the bit error ratio performance of various types of modulated signals, with and without error correction coding and with and without channel fading, were obtained by simulation and the results compared with those obtained analytically when possible. In the next chapter, conclusions are drawn and suggestions for future work made.

# V. CONCLUSION AND FUTURE WORK

## A. CONCLUSION

Using SystemView, we simulated the effect of various types of fading channels. Two major problems were found during the modeling and simulation. First, the total number of computations is restricted on each simulation loop, which limits the degree of accuracy for high SNR. Next, too much CPU resource is required for each simulation, and it is time consuming to accurately simulate performance for high SNR. Presumably, using the commercial version instead of the student version would alleviate these difficulties.

Except for these two problems, generally speaking, SystemView provides a good modeling and simulation tool for communication systems. The performance of coherent systems with no coding, the performance of coherent systems with coding, and the performance of coherent systems with no coding and fading channels all agree very well with analytical results. Most importantly, the performance of communication systems affected by narrowband noise and other channel impairments that are difficult to analyze are easily simulated in SystemView. Since the simulations developed have been verified for the AWGN case, they can now be modified to examine cases that are not possible to evaluate by analysis.

## B. FUTURE WORK

With rapid progress in hardware and software, the simulation process will be significantly improved. The utility of this simulation tool for evaluating difficult to analyze systems has been demonstrated, and SystemView can be used to evaluate any number of modern communication systems. The combination of error correction coding and modulation specified by the various digital standards, such as *IEEE* 802.11*g*, should be examined for fading channels and interference conditions other than simple AWGN to foster improved understanding of how these popular communications wireless standards perform in various radio environments. For example, the barrage noise jamming considered in Chapter IV is simply additional AWGN. It would be valuable to re-

examine this case, but for a barrage noise jammer implemented by frequency modulating a voltage controlled power oscillator using bandlimited AWGN or bandlimited AWGN plus a periodic waveform, as is typical of real military electronic warfare systems [19].

# LIST OF REFERENCES


1 L. Wan, and V.K. Dubey, "Bit Error Probability of OFDM System Over Frequency-nonselective Fast Rayleigh Fading Channels," *IEEE Electronics Letters*, Vol. 36, pp. 1306-07, 15 July 2000.

2 L. Wan, and V.K. Dubey, "BER Performance of OFDM System Over Frequency-nonselective Fast Ricean Fading Channels," *IEEE Electronics Letters*, Vol. 5, pp. 19-21, 1 January 2001.

3 David A. Wiegandt & Carl R. Nassar, "High-Performance 802.11a Wireless LAN via Carrier-Interferometry Orthogonal Frequency Division Multiplexing at 5GHz," *IEEE Global Telecommunications Conference 2001*, Vol. 6, pp. 3579-3582.

4 Chi-han Kao, "Performance of the IEEE 802.11a Wireless LAN standard over Frequency-selective, Slow, Ricean Fading Channels," Master's Thesis, Naval Postgraduate School, Monterey, CA, 2002.

5 Patrick A. Count, "Performance Analysis of OFDM in Frequency-selective, Slowly Fading Nakagami Channels," Master's Thesis, Naval Postgraduate School, Monterey, CA, 2001.

6 Kosa Irfan, "Performance of IEEE 802.11a Wireless LAN Standard over Frequency-selective, slowly fading Nakagami Channels in a pulsed jamming environment," Master's Thesis, Naval Postgraduate School, Monterey, CA, 2002.

7 John G. Proakis, *Digital Communications*, 4th edition, McGraw-Hill Book Co., New York, 2001

8 C.E. Shannon, "A Mathematical Theory of Communications," *Bell Systems Technical Journal*, Vol. 27, pp. 379-423 and 623-656, 1948

9 R. Clark Robertson, Notes for EC4580 (Error correction coding), Naval Postgraduate School, Monterey, CA, 2002 (unpublished).

10 W.Y.C. Lee, *Mobile Cellular Communication*, McGraw-Hill Book Co., New York, 1989.

11 B. Sklar, *Digital Communications: Fundamentals And Applications*, 2nd edition, Prentice Hall, Upper Saddle River, NJ, 2001.

12 Mike Fitton, Principles of Digital Modulation, Telecommunications Research Lab, http://wireless.ictp.trieste.it/school_2002/lectures/fitton/digital_mod.pdf, accessed on 10/27/05.

13 Alan Triggs, Notes for Wireless, Cellular, & Personal Telecommunications, Lecture 7, Southern Methodist University, Fall 2001, http://engr.smu.edu/~triggs/EETS8306_Lecture7_Prop&Fading&Budgets&coverage2perpage.PDF, accessed on 10/27/03.

14 T. S. Rappaport, *Wireless Communications Principles and Practice*, 2nd edition, Prentice Hall, Upper Saddle River, NJ, 2002.

15 R. Clark Robertson and Nathan Beltz, "Digital Communication over Fading Channels," Technical Report, Naval Postgraduate School, Monterey, CA, 2004.

16 S. Lin and D. J. Costello, Jr., *Error control coding: fundamentals and applications*, Prentice Hall, Englewood Cliffs, NJ, 1983.

17 J. P. Odenwalder, "Optimum decoding of convolutional codes," Ph. D. dissertation, University of California, Los Angeles, 1970.

18 Institute of Electrical and Electronics Engineers, 802.11a, *Wireless LAN Medium Access Control (MAC) and Physical Layer (PHY) Specifications: High-Speed Physical Layer Extension in the 5 GHz Band*, 16 September 1999.

19 Radar training system model 8096, Lab-Volt. http://www1.labvolt.com/publications/Datasheets/Current2/dsa8096.pdf, accessed on 3/30/07

# INITIAL DISTRIBUTION LIST

1. Defense Technical Information Center
   Ft. Belvoir, Virginia

2. Dudley Knox Library
   Naval Postgraduate School
   Monterey, California

3. Chairman, Code EC
   Department of Electrical and Computer Engineering
   Naval Postgraduate School
   Monterey, California

4. Professor Clark Robertson, Code EC/RC
   Department of Electrical and Computer Engineering
   Naval Postgraduate School
   Monterey, California

5. Assistant Professor Frank Kragh, Code EC/Kh
   Department of Electrical and Computer Engineering
   Naval Postgraduate School
   Monterey, California

6. Der-Hung Kong
   No. 26, Lane 35, Guangdung 2nd St.
   Kaohsiung, Taiwan 802, R.O.C